Development Advance Online Articles. First posted online on 15 May 2017 as 10.1242/dev.150490
Access the most recent version at http://dev.biologists.org/lookup/doi/10.1242/dev.150490

MAPK pathway activation in the embryonic pituitary results in stem cell compartment expansion, differentiation defects and provides insights into the pathogenesis of papillary craniopharyngioma

S. Haston[1], S. Pozzi[1], G. Carreno[1], S. Manshaei[1], L. Panousopoulos[1], J.M. Gonzalez-Meljem[1], J.R. Apps[1], A. Virasami[2], S. Thavaraj[3], A. Gutteridge[4], T. Forshew[4], R. Marais[5], S. Brandner[6,7], T.S. Jacques[1,2], C.L Andoniadou[8,9] and J.P. Martinez-Barbera[1*]

1. Developmental Biology and Cancer Programme, Birth Defects Research Centre, Great Ormond Street Institute of Child Health, University College London, London, UK
2. Department of Histopathology, Great Ormond Street Hospital for Children NHS Foundation Trust, London, UK
3. Head and Neck Pathology, Dental Institute, King's College London, London, UK
4. Department of Pathology, UCL Cancer Institute, London UK
5. Molecular Oncology Group, Cancer Research UK Manchester Institute, The University of Manchester, Manchester, UK
6. Department of Neurodegenerative Disease, UCL Institute of Neurology, Queen Square, London, UK
7. Division of Neuropathology, The National Hospital for Neurology and Neurosurgery, Queen Square, London, UK
8. Craniofacial Development and Stem Cell Biology, Dental Institute, King's College London, London, UK
9. Department of Internal Medicine III, Technische Universität Dresden, Dresden, Germany

* Corresponding author: j.martinez-barbera@ucl.ac.uk

Key words: Pituitary, development, mouse, papillary craniopharyngioma, Sox2, tumour.

SUMMARY STATEMENT

This research demonstrates that the MAPK/ERK pathway controls the balance between proliferation and differentiation of embryonic precursors and identifies a potential mechanism underlying the pathogenesis of papillary craniopharyngioma.

ABSTRACT

Despite the importance of the RAS-RAF-MAPK pathway in normal physiology and disease of numerous organs, its role during pituitary development and tumourigenesis remains largely unknown. Here we show that the over-activation of the MAPK pathway, through conditional expression of the gain-of-function alleles *BrafV600E* and *KrasG12D* in the developing mouse pituitary, results in severe hyperplasia and abnormal morphogenesis of the gland by the end of gestation. Cell-lineage commitment and terminal differentiation are disrupted, leading to a significant reduction in numbers of most of the hormone-producing cells before birth, with the exception of corticotrophs. Of note, Sox2+ve stem cells and clonogenic potential are drastically increased in the mutant pituitaries. Finally, we reveal that papillary craniopharyngioma (PCP), a benign human pituitary tumour harbouring *BRAF p.V600E* also contains Sox2+ve cells with sustained proliferative capacity and disrupted pituitary differentiation. Together, our data demonstrate a critical function of the MAPK pathway in controlling the balance between proliferation and differentiation of Sox2+ve cells and suggest that persistent proliferative capacity of Sox2+ve cells may underlie the pathogenesis of PCP.

INTRODUCTION

In vertebrates, the pituitary gland is considered to be master regulator of homeostasis because it regulates a wide range of essential physiological functions such as metabolism, growth, fertility and the stress response. The pituitary gland comprises anterior, intermediate and posterior lobes (AL, IL, and PL, respectively). The AL and IL derive from Rathke's pouch, a dorsal evagination of the oral ectoderm at the boundary with the pharyngeal endoderm. The PL develops from a diverticulum at the ventral midline of the diencephalon, the infundibulum. At 18.5 dpc, the AL contains five hormone-expressing cell types: somatotrophs, lactotrophs, thyrotrophs, gonadotrophs and corticotrophs, which secrete growth hormone (GH), prolactin (PRL), thyroid-stimulating hormone (TSH), gonadotropins (FSH and LH) and adrenocorticotropin hormone (ACTH), respectively (Kelberman et al., 2009). In addition, the AP contains Sox2+ve/Sox9+ve cells, a proportion of which represent stem cells in the postnatal pituitary (Castinetti et al., 2011; Andoniadou et al., 2013; Rizzoti et al., 2013). These cells are concentrated around the pituitary cleft in the IL and the "marginal zone", a region of the dorsal AL mostly devoid of hormone-producing cells (Fauquier et al., 2008; Garcia-Lavendeira et al., 2009; Goldsmith et al., 2016; Perez-Millan et al., 2016). Dispersed Sox2+ve/Sox9+ve cells are also detected throughout the parenchyma of the AL, intermingled with hormone-expressing cells (Mollard et al., 2012). The IL contains melanotrophs, which express melanocyte-stimulating hormone (MSH). The PL is devoid of endocrine cell types and contains the axonal projections from hypothalamic neurons.

Several signalling pathways and transcription factors regulate the normal development of the pituitary gland. Around 9.5 days post coitum (dpc), secreted signals from the prospective hypothalamus such as FGF8, FGF10, BMP4 and SHH are required for RP induction and for the expression of transcription factors including *Hesx1*, *Sox2*, *Lhx3* and *Lhx4* in RP progenitors (Ericson et al., 1998; Treier et al., 1998; Treier et al., 2001). RP

progenitors divide actively from 9.5 to 14.5 dpc (Davis et al., 2011) to generate post-mitotic precursors that initiate cell-lineage commitment by expressing: (i) Sf1 (*Nr5a1*), in the gonadotroph cell lineage (Schimmer and White, 2010), (ii) The T-box transcription factor Tpit, responsible for the activation of the proopiomelanocortin (*Pomc1*) gene in corticotrophs (and melanotrophs of the intermediate lobe) (Lamolet et al., 2001) and (iii) POU Class 1 homeobox 1 (Pou1f1 or Pit1), which control the differentiation of thyrotrophs, lactotrophs and somatotrophs (Dolle et al., 1990). Mouse mutants and humans carrying inactivating mutations in most of these genes develop hypopituitarism (Fang et al., 2016).

The mitogen-activated protein kinase (MAPK) pathway encompasses different signalling cascades, of which the Ras-Raf-Mek-ERK1/2 (hereafter MAPK/ERK) is one of the most dysregulated in human cancer and additionally, plays important roles during normal physiology (Dhillon et al., 2007) (Zhang and Liu, 2002). Extracellular growth factors (FGFs, EGF and PDGF among others) bind to and activate receptor tyrosine kinases, causing a downstream phosphorylation cascade (RAS-RAF-MEK-ERK), which eventually leads to transcription of target genes controlling cellular proliferation, differentiation, apoptosis and senescence. Gain-of-function mutations in components of the pathway, such as *BRAF p.V600E* and *KRAS p.G12D*, have been identified in numerous tumours and cancers (Dhillon et al., 2007). These mutations lead to the over-activation of the MAPK/ERK pathway and increase cell proliferation and survival, resulting in cell transformation and tumourigenesis. In pituitary tumours, biochemical evidence indicates that this pathway is activated in many types of pituitary adenoma in humans (Dworakowska et al., 2009). However, mutations in components of the pathway have been identified only in papillary craniopharyngioma (PCP); specifically the *BRAF p.V600E* mutation is present in the vast majority of the tumours analysed (Brastianos et al., 2014).

In this manuscript, we have addressed the role of MAPK/ERK pathway during normal pituitary development and in tumourigenesis by conditionally activating this pathway in RP progenitors during embryonic development. Our results demonstrate that persistent activation of the pathway leads to a drastic increase in the proliferative capacity of Sox2+ve cells and impairment of their differentiation properties resulting in enlargement of the Sox2+ve stem cell compartment by the end of gestation. Additionally, expression analysis of human tumour samples strongly suggests that similar mechanisms underlie the pathogenesis of PCP.

RESULTS

Severe anterior lobe hyperplasia and neonatal lethality in *Hesx1*$^{Cre/+}$;*Braf*$^{V600E/+}$ and *Hesx1*$^{Cre/+}$;*Kras*$^{G12D/+}$ mutants

We have previously shown that the *Hesx1-Cre* mouse line drives robust Cre-mediated activity in the developing pituitary gland by 9.0 dpc (Andoniadou et al., 2007; Gaston-Massuet et al., 2011; Jayakody et al., 2012). To assess the role of the MAPK/ERK pathway during development, we crossed the *Hesx1*$^{Cre/+}$ mice with either *Braf*$^{V600E/+}$ or *Kras*$^{G12D/+}$ animals (Jackson et al., 2001; Dhomen et al., 2009). Genotypic analysis of 10.5-18.5 dpc embryos showed no statistically significant variation from the expected Mendelian ratios (**Supplementary Table 1**). In contrast, genotyping of postnatal mice from birth to 3 weeks failed to identify any viable *Hesx1*$^{Cre/+}$;*Braf*$^{V600E/+}$ or *Hesx1*$^{Cre/+}$;*Kras*$^{G12D/+}$ mice (**Supplementary Table 1**). Histological examination revealed the presence of expanded airway structures in both mouse models at 18.5 dpc, suggesting that abnormal lung development could be the cause of the perinatal death observed (**Supplementary Fig. 1**) (Tang et al., 2011).

Haematoxylin-eosin staining of *Hesx1*$^{Cre/+}$;*Braf*$^{V600E/+}$ and *Hesx1*$^{Cre/+}$;*Kras*$^{G12D/+}$ mutants at 10.5 dpc revealed no gross morphological defects in the developing RP of these mutants compared with control littermates (**Fig. 1A-C**). The first clear evidence of a morphological defect, typically anterior pituitary hyperplasia, was observed at 12.5 dpc and further pronounced by 14.5 dpc (**Fig. 1D-I**). At 18.5 dpc, a fully penetrant phenotype of severe anterior pituitary hyperplasia with branched cleft was observed in all embryos analysed (**Fig. 1J-L**). Cell counts of dissociated pituitaries at 18.5 dpc revealed a total of 96000 ± 2.7% in the *Hesx1*$^{Cre/+}$;*Braf*$^{V600E/+}$mutant (p=<0.01), 101666 ± 4.3% in the *Hesx1*$^{Cre/+}$;*Kras*$^{G12D/+}$ mutant (p=<0.01) and 67200 ± 3.5% in control wild-type mice (**Fig. 1M**). The posterior lobe was present and apparently normal in *Hesx1*$^{Cre/+}$;*Braf*$^{V600E/+}$ and *Hesx1*$^{Cre/+}$;*Kras*$^{G12D/+}$ mutant pituitaries (**Fig. 1J-L**). These data suggest that RP induction occurs normally in the *Hesx1*$^{Cre/+}$;*Braf*$^{V600E/+}$ and *Hesx1*$^{Cre/+}$;*Kras*$^{G12D/+}$ mutants, followed by an increase in proliferation, leading to hyperplasia of the anterior pituitary by the end of gestation.

The MAPK/ERK pathway is regulated temporally and spatially during normal pituitary development

The expression pattern of *Braf* and *Kras* mRNA and pERK1/2 protein expression, as a readout of activated MAPK/ERK pathway, were respectively analysed by *in situ* hybridisation and immunostaining, on histological sections of wild-type, *Hesx1*$^{Cre/+}$;*Braf*$^{V600E/+}$ and *Hesx1*$^{Cre/+}$;*Kras*$^{G12D/+}$ embryos.

At 10.5 dpc wild-type embryos, *Braf* and *Kras* mRNA were clearly detected in the prospective hypothalamus, including the posterior diencephalon and pre-optic area, in addition to the developing RP (**Fig. 2A,D**). At 12.5 and 14.5 dpc, transcripts were detected throughout the developing pituitary, including the infundibulum, periluminal epithelium and

anterior lobe (**Figure 2B,E; data not shown**). At 18.5 dpc, the expression domain of *Kras* and *Braf* was restricted to the periluminal area including the intermediate lobe and marginal zone with scattered cells dispersed throughout the anterior lobe (**Fig. 2C,F**). The expression patterns of *Braf* in *Hesx1*$^{Cre/+}$;*Braf*$^{V600E/+}$ (**Fig. 3A-C**) and *Kras* in *Hesx1*$^{Cre/+}$;*Kras*$^{G12D/+}$ (data not shown) mutants were comparable to those in wild-type embryos.

These expression patterns of mRNA expression did not correlate with pERK1/2 detection at all embryonic stages. At 10.5 dpc, pERK1/2 expression was comparable between genotypes in both the developing hypothalamus and RP (**Fig. 4A,E,I**), corresponding with the *Braf* and *Kras* mRNA expression (**Fig. 2**). In contrast, at 12.5 and 14.5 dpc, very few pERK1/2+ve cells were detected, despite the broad expression of *Braf* and *Kras* mRNA in mutant and wild-type embryos (**Fig. 4B,C,F,G,J,K**) as well as the extensive expression of BRAF-V600E mutant protein throughout the *Hesx1*$^{Cre/+}$;*Braf*$^{V600E/+}$ pituitary (**Fig. 3D-F**). At 18.5 dpc, the expression of pERK1/2 was noticeably increased in both *Hesx1*$^{Cre/+}$;*Braf*$^{V600E/+}$ and *Hesx1*$^{Cre/+}$;*Kras*$^{G12D/+}$ mutants compared with the control pituitaries (**Fig. 4D,H,L**) and correlated with the *in situ* data (**Fig. 2 and 3; data not shown**). Together, these expression studies demonstrate that the MAPK/ERK pathway is temporally regulated with the highest levels observed at 10.5 and 18.5 dpc. In addition, we show that most of the cells up-regulating the pathway are located in the epithelium lining the cleft, an area enriched for Sox2+ve undifferentiated embryonic precursors and stem cells (Andoniadou et al., 2013).

Over-activation of the MAPK/ERK pathway results in abnormal terminal differentiation of specific hormone-producing cells

To assess the effects of the over-activation of the MAPK/ERK pathway in Rathke's pouch (RP) induction, cell lineage commitment and terminal differentiation, we performed detailed expression analyses at 10.5, 14.5 and 18.5 dpc in both mutants in comparison with controls.

The expression of *Fgf10*, *Bmp4* and *Shh* within the hypothalamus is required for *Lhx3* activation in RP progenitors (Ericson et al., 1998; Treier et al., 1998; Treier et al., 2001). At 10.5 dpc, the expression domains of these markers were indistinguishable between mutants and controls, supporting the notion that early RP induction occurs normally in the *Hesx1*$^{Cre/+}$*;Braf*$^{V600E/+}$ and *Hesx1*$^{Cre/+}$*;Kras*$^{G12D/+}$ mutant embryos (**Supplementary Fig. 2**). Immunostaining against POU1F1 (PIT1), NR5A1 (SF1) and TPIT, markers of specific cell-lineage precursors of the anterior pituitary, revealed evident defects in the *Hesx1*$^{Cre/+}$*; Braf*$^{V600E/+}$ mutants relative to control embryos at 14.5 dpc (**Fig. 5A-I**). Specifically, the proportion of PIT1+ve cells were significantly reduced relative to total cells (control, 29%, *Braf* mutant, 4%, p=0.001), SF1+ve cells were almost absent (control, 4%; *Braf* mutant, 0.5%; p=<0.05) and TPIT+ve cells were increased (control, 10%; *Braf* mutant, 26%; p=0.001) (**Fig. 5J**). In the *Hesx1*$^{Cre/+}$*;Kras*$^{G12D/+}$ mutants, PIT1+ve and SF1+ve cell lineage precursors were also significantly reduced (PIT1+ve: control, 29%; *Kras* mutant, 13%; p=<0.01; SF1+ve: control, 4.5%; *Kras* mutant, 0.6%; p=<0.05), albeit to a lesser extent than in *Hesx1*$^{Cre/+}$*;Braf*$^{V600E/+}$mutants. Numbers of TPIT+ve cells were similar (control, 10%; *Kras* mutant, 12%; p=0.6156) (**Fig. 5J**).

Total numbers of hormone-producing cells were calculated by adjusting the proportion of each of these cell types to the size of the pituitary gland of the *Hesx1*$^{Cre/+}$*;Braf*$^{V600E/+}$, *Hesx1*$^{Cre/+}$*;Kras*$^{G12D/+}$ and control embryos at 18.5 dpc (See Materials and Methods). We reasoned that this approach could avoid any bias in the quantitative analysis due to the hyperplasia observed in the mutant pituitaries; for instance, numbers of a particular cell type could be the same in mutant and controls but distributed in more histological sections in the mutant pituitary, hence seeming proportionally reduced. Overall, specific immunostaining revealed abnormal terminal differentiation of hormone-producing cells in both *Hesx1*$^{Cre/+}$*;Braf*$^{V600E/+}$ and *Hesx1*$^{Cre/+}$*;Kras*$^{G12D/+}$ mutants, although the effects

were more accentuated in the former (**Fig. 6A-R**). Specifically, numbers of somatotrophs (GH+ve) (WT - 23560, *Braf* mutant - 3185), lactotrophs (PRL+ve) (WT - 17604, *Braf* mutant - 3233) and thyrotrophs (TSH+ve) (WT - 4043, *Braf* mutant - 664) (i.e. the *Pit1* cell-lineage) were significantly reduced, and gonadotrophs (FSH+ve) (WT - 6134, *Braf* mutant - 1686) and LH+ve (WT - 1564, *Braf* mutant - 23) almost completely absent in *Hesx1*$^{Cre/+}$;*Braf*$^{V600E/+}$ mutant pituitaries relative to controls (**Fig. 6S**). Immunostaining against αGSU (WT - 6861, *Braf* mutant - 2977) confirmed the reduction of thyrotrophs and gonadotrophs in the mutant pituitaries **(Supplementary Fig. 3)**. In contrast, total numbers of corticotrophs (ACTH+ (WT - 15958, *Braf* mutant - 28778) appeared significantly elevated in *Hesx1*$^{Cre/+}$;*Braf*$^{V600E/+}$ mutants (**Fig. 6S**). Abnormal differentiation was also observed in the *Hesx1*$^{Cre/+}$;*Kras*$^{G12D/+}$ mutant pituitaries, but to a lesser extent, with a reduction in numbers of thyrotrophs (WT - 4043, *Kras* mutant -1371), gonadotrophs (FSH+ve (WT - 6134, *Kras* mutant - 4044) and lactotrophs (WT -17604, *Kras* mutant - 6710). Similar to *Hesx1*$^{Cre/+}$;*Braf*$^{V600E/+}$ mutants, elevated numbers of corticotrophs were also observed in *Hesx1*$^{Cre/+}$;*Kras*$^{G12D/+}$ mutant pituitaries (WT – 15958, *Kras* mutant - 21370) (**Fig. 6S**). Furthermore, absolute quantification of mRNA transcripts using quantitative RT-PCR from 18.5 dpc control, *Hesx1*$^{Cre/+}$;*Kras*$^{G12D/+}$and *Hesx1*$^{Cre/+}$;*Braf*$^{V600E/+}$ pituitaries revealed a significant decrease in *Gh* and a trend towards increased *Acth* mRNA in both mutant genotypes (**Fig. 6T**), in agreement with the cell counts.

Together, these analyses demonstrate that cell-lineage commitment and terminal differentiation are severely disrupted upon activation of the MAPK pathway in RP embryonic precursors, with an overall reduction of hormone-producing cells at the end of gestation.

Increased proliferation of the developing pituitary in *Hesx1$^{Cre/+}$;Braf$^{V600E/+}$* and *Hesx1$^{Cre/+}$;Kras$^{G12D/+}$* embryos

Analysis of cell proliferation of RP progenitors was carried out at 12.5, 14.5 and 18.5 dpc in *Hesx1$^{Cre/+}$;Braf$^{V600E/+}$*, *Hesx1$^{Cre/+}$;Kras$^{G12D/+}$* and control pituitaries. Quantitative analysis of the proliferation index using Ki67 staining, a marker of cycling cells, revealed no difference at 12.5 dpc, with around 70% of total cells being Ki67+ve (**Fig. 7A-C, J**). However, a significant increase in Ki67+ve cells at 14.5 and 18.5 dpc was observed in both mutant genotypes, relative to stage-matched controls (**Fig. 7D-J**). Of note, while the Ki67 proliferation index decreased gradually in control pituitaries from 72% at 12.5 dpc to 22% at 18.5 dpc, this progressive quiescence was not observed to the same degree in the *Hesx1$^{Cre/+}$;Kras$^{G12D/+}$* or *Hesx1$^{Cre/+}$;Braf$^{V600E/+}$* mutants. At 18.5 dpc, the proportion of proliferating cells fell to only 42% in *Hesx1$^{Cre/+}$;Kras$^{G12D/+}$* and 55% in *Hesx1$^{Cre/+}$;Braf$^{V600E/+}$* mutant pituitaries (**Fig. 7J**). Increased proliferation was also confirmed by immunostaining against Cyclin D2, which controls G1/S cell cycle progression and is mainly expressed in RP progenitors in the periluminal epithelium (Bilodeau et al., 2009). Quantification of Cyclin D2-expressing cells out of total DAPI-stained nuclei within the periluminal epithelium revealed an increased trend in both mutant genotypes at 12.5 dpc compared with stage-matched controls (**Supplementary Fig. 4**).

Activation of the MAPK/ERK pathway results in expansion of the Sox2 stem cell compartment

The restricted expression of pERK1/2 and increased proliferation of periluminal cells, prompted us to assess whether the Sox2+ve cells could be the main population responding to the over-activation of the MAPK/ERK pathway in our mouse models. Histological sections

of *Hesx1*$^{Cre/+}$;*Braf*$^{V600E/+}$, *Hesx1*$^{Cre/+}$;*Kras*$^{G12D/+}$ and control pituitaries were analysed by immunostaining at different developmental stages. At 12.5 dpc the proportion of Sox2+ve cells was initially similar between genotypes at around 80% of total cells (**Fig. 8A-C, J**). However, in control embryos numbers of Sox2+ve cells fell to 21% by 18.5 dpc (p=0.0004) (**Fig. 8G, J**). Strikingly, in *Hesx1*$^{Cre/+}$;*Kras*$^{G12D/+}$ and *Hesx1*$^{Cre/+}$;*Braf*$^{V600E/+}$ mutant pituitaries the high proportion of Sox2+ve cells found at earlier developmental time points was maintained, falling to only 53% (p=0.0519) and 72% (p=0.068) of total cells at 18.5 dpc, respectively. This suggests a trend towards a decrease in Sox2+ve cell numbers although not statistically significant (**Fig. 8H-J**). Further to this, levels of *Sox2* mRNA were observed to be significantly increased in *Hesx1*$^{Cre/+}$;*Braf*$^{V600E/+}$mutants by quantitative RT-PCR (**Fig. 8K**). Corroborating the histological findings, the clonogenic potential in *Hesx1*$^{Cre/+}$;*Kras*$^{G12D/+}$ and *Hesx1*$^{Cre/+}$;*Braf*$^{V600E/+}$ pituitaries at 18.5 dpc was nearly three and five times higher, respectively, than in controls when analysed in stem cell promoting medium (**Fig. 8L,M**).

The described defects suggest that the MAPK pathway may control the balance between self-renewal and differentiation of Sox2+ve progenitors during development. To further characterise this defect, we performed a pulse chase experiment with the nucleotide analogue EdU, which is incorporated during the S phase of the cell cycle. Specifically, we injected EdU at 14.5 dpc, when most of the replicating cells are Sox2+ve progenitors and analysed the pituitaries 48 hours later at 16.5 dpc, when progenitors have exited cell cycle to commit to specific cell lineages (Fauquier et al., 2008; Bilodeau et al., 2009). This was performed in both control and *Hesx1*$^{Cre/+}$;*Braf*$^{V600E/+}$embryos, due to their more pronounced phenotype.

In control embryos, approximately 25% of the initially labelled EdU cells expressed the commitment marker PIT1 and around 21% expressed SOX2 (**Fig. 9A, C, D,F**). In

contrast, in *Hesx1*$^{Cre/+}$;*Braf*$^{V600E/+}$ mutants, the percentage of EdU+/PIT1+ cells dropped to 3% and the proportion of EdU+/Sox2+ cells was elevated to 40% (**Fig. 9B,C,E,F**). Despite the significant increase in ACTH+ve cells in the mutant pituitary at 18.5 dpc, the proportion of EdU+/TPIT+ positive in this tracing experiment remained similar between genotypes (8% in controls and 9% in mutants) **(Fig. 9H-I)**. This tracking experiment also revealed a higher proportion of EdU+/Ki67+ cells in the *Hesx1*$^{Cre/+}$;*Braf*$^{V600E/+}$ mutants (25%) relative to the controls (18%) (**Fig. 9J-L**). To assess which cells were labelled at 14.5 dpc, we performed a short pulse experiment by injecting EdU in pregnant females at 14.5 dpc and analysed the embryos 2 hours later. This analysis confirmed the majority of the EdU+ cells expressed SOX2, specifically 74% of labelled EdU+ cells expressed SOX2 in the control and 87% in the *Hesx1*$^{Cre/+}$;*Braf*$^{V600E/+}$ mutants pituitaries, suggesting a trend towards an increase although not significant (p=0.1599) **(Supplementary Fig. 5A-C)**. In the control pituitary, 6% of the EDU+ cells expressed PIT1 and 1.4% TPIT, whilst in the mutant pituitary these proportions were 0.1% for PIT1 and 3.7% for TPIT, both significantly different (p=0.0246, PIT1 and p=0.0490, TPIT) **(Supplementary Fig. 5D-I)**. Three conclusions can be drawn from these EdU studies: (i) the activation of the MAPK/ERK pathway drives self-renewal versus differentiation of Sox2+ve cells; (ii) there is a blockade in the differentiation of Sox2+ve cells into PIT1 progenitors; (iii) there is no bias in the differentiation of Sox2+ve cells into the TPIT cell lineage; rather TPIT progenitor respond to the pathway activation by increasing proliferation. Together, these data demonstrate that the activation of the MAPK pathway in embryonic precursors results in significant expansion of the Sox2+ve cell population and increased clonogenic potential. In addition, we show that an abnormal balance between self-renewal and differentiation contribute to these defects.

Sox2+ve cells represent the major proliferating cell population in human papillary craniopharyngioma

Higher numbers of organ-specific stem cells with reduced differentiation potential can lead to tumourigenesis in many organs including the pituitary gland (Gaston-Massuet et al., 2011). As *BRAF p.V600E* is the sole genetic event associated with human papillary craniopharyngioma (PCP), we hypothesised that over-activated MAPK in these tumours may lead to similar cellular alterations to those observed in the $Hesx1^{Cre/+};Braf^{V600E/+}$ mutant pituitary, i.e. expansion of the Sox2/Sox9+ve cells with decreased differentiation capacity.

PCPs are histologically characterised by the presence of cores of fibrovascular stroma lined by basal cells and suprabasal layers of well-differentiated non-keratinised squamous epithelium (**Fig. 10A**). PCPs are non-functional tumours, which do not express pituitary hormones (Louis et al., 2016). In a series of archival FFPE PCP specimens (n=5), we confirmed the presence of p.BRAF(V600E) mutations (**Supplementary Table 2**) and expression of BRAFV600E in all tumour cells (**Fig. 10B;** light brown staining). pERK1/2 staining was more restricted and focused in areas around the fibrovascular cores (**Fig. 10E**). Most of the cells in the tumours were positive against a pan-cytokeratin antibody recognising cytokeratins, but cells from the basal layer were negative (**Fig. 10C;** dark brown staining). This was further evidenced by immunostaining against cytokeratin 19 (**Fig. 10D;** light brown staining). Double immunostaining revealed that the squamous epithelial tumour components robustly expressed SOX2 and SOX9 in a graded manner, with the highest expression observed in basal cells immediately in contact with the fibrovascular cores and a progressive loss of signal in cells away from the SOX2+/SOX9+ve areas (**Fig. 10F-H**). Quantification analyses demonstrated that approximately 16% of these Sox2+ve cells expressed Ki67 (**Fig. 10I-L**). Moreover, up to 91% of all cycling cells within the tumour (excluding host-derived

stroma) co-expressed SOX2, suggesting that proliferating SOX2+ve cells may be driving PCP growth (**Fig. 10L**).

For comparison purposes, we assessed the proliferative potential of Sox2+ve cells during normal human embryonic pituitary development and adulthood. At CS20 (Carnegie stage 20; gestational day 49), an embryonic stage that is analogous to 14.5 dpc in mouse, human fetal pituitaries were predominantly SOX2;SOX9+ve and almost the majority of these cells expressed Ki67 (**Supplementary Fig. 6A-C,J-L**). In contrast, adult human pituitary samples contained very few SOX2+ve cells in the anterior lobe (**Supplementary Fig. 6D-I**), which very rarely expressed Ki67 with an almost mutual exclusivity between these two markers (**Supplementary Fig. 6M-R**). These observations suggest that, as in the mouse model, the activation of the MAPK pathway in human PCP tumours result in increased proliferative capacity and reduced terminal differentiation of the Sox2+ve cells.

DISCUSSION

In this manuscript we show that the over-activation of the MAPK pathway in RP embryonic precursors results in increased, sustained proliferation and impaired terminal differentiation of Sox2+ve cells during development. Consequentially, by the end of gestation, the pituitary gland contains vast numbers of Sox2+ve cells leading to an enlargement of the pituitary stem cell compartment. Because the *Hesx1-Cre* mouse line drives Cre-mediated recombination in the anterior hypothalamus, we cannot completely rule out a hypothalamic contribution to the observed phenotype. However, the normal hypothalamic patterning at 10.5 dpc supports a more relevant role for the dysregulation of the MAPK/ERK pathway in the developing RP. Of translational relevance, we reveal the presence of a population of Sox2+ve cells in human

PCP tumours bestowed of proliferating capacity but unable to differentiate into hormone-producing pituitary cells.

Our data suggest that the activation of the MAPK/ERK pathway by FGF ligands is critical during pituitary development. The FGF family of secreted factors binds to tyrosine kinase FGF receptors (FGFRs) to signal through the MAPK/ERK and other pathways (Ornitz and Itoh, 2015). Several FGFs including *Fgf8, 10* and *18* are expressed in the developing ventral diencephalon around 9.5-10.5 dpc (Treier et al., 1998; Treier et al., 2001) and loss-of-function mutants of FGF and FGFR2, demonstrate that FGF signalling is required for normal proliferation of RP progenitors and pituitary morphogenesis (De Moerlooze et al., 2000; Ohuchi et al., 2000). Ex vivo culture of RP tissue exposed to FGFs and FGF inhibitors has revealed a critical function for the pathway in controlling both RP proliferation and, its down-regulation is required for normal PIT1-cell lineage specification (Ericson et al., 1998; Norlin et al., 2000). Of note, transgenic ectopic expression of *Fgf8* in the developing pituitary using a Cga (a-GSU) promoter results in pituitary hyperplasia and expansion of ACTH-expressing cells (corticotrophs and melanotrophs) with a concomitant severe loss of gonadotrophs, somatotrophs, thyrotrophs and gonadotrophs (Treier et al., 1998), a phenotype resembling our mouse models activating the MAPK-ERK pathway. The data presented here open the possibility that other ligands such as EGF, PDGF and TGFα, which, like FGFs can activate the MAPK/ERK pathway, may be important during pituitary development. Alternatively, it is also possible that FGF is the only secreted signal activating the MAPK/ERK pathway in RP. Further analyses are required to clarify the contributions of other signals besides FGFs.

We reveal a critical function of the MAPK/ERK pathway in the control of the stem cell compartment in the pituitary by the end of gestation. The proportion of Sox2+ve cells is drastically increased and comprises almost ¾ of the entire cell population in the *Hesx1*$^{Cre/+}$*;Braf*$^{V600E/+}$ at 18.5 dpc. Our analyses show that this substantial expansion is due to

a failure of Sox2+ve embryonic progenitors to exit cell cycle and differentiate at earlier developmental stages, resulting in increased clonogenic potential by the end of gestation. In addition, pERK1/2 staining is strongly detected in the marginal zone, a region enriched in Sox2+ve stem cells at 18.5 dpc, suggesting that the MAPK pathway has a role in controlling stem cell specification during development and perhaps during stem cell homeostasis postnatally.

BRAF and *KRAS* mutations are uncommon in pituitary adenomas (Newey at al., 2013; Reincke et al., 2015; Ronchi et al., 2016; Välimäki et al., 2015), but the over-activation of the MAPK/ERK pathway has been reported in these neoplasias. A mutation was identified in codon 12 of the *HRAS* gene (Gly to Val) in a recurrent prolactinoma that was highly invasive and ultimately proved to be fatal (Karga et al., 1992). Over-expression of both BRAF mRNA and protein has also been reported in non-functioning pituitary adenomas (Ewing et al., 2007). Persistent MAPK/ERK pathway activation, by expressing oncogenic KRAS-G12V, promotes differentiation of the bi-hormonal somatolactotroph GH4 precursor cell line into a prolactin-secreting cell type but is not sufficient to drive tumourigenesis (Booth et al., 2014). In our mouse models, lactotroph differentiation is impaired rather than promoted, suggesting that cell context where the MAPK/ERK pathway is activated (i.e. GH4 versus embryonic precursors) and/or approach used (i.e. *in vitro* versus *in vivo*) may have a profound effect on the phenotypic outcomes.

PCPs are benign tumours of the sellar region, mostly affecting the elderly, and can be associated with significant morbidity when behaving aggressively. The majority of the PCP tumours carry *BRAF p.V600E* mutations, but little is known about the consequences of the expression of this oncogenic protein (Brastianos et al., 2014). Of interest, preliminary data indicate that the use of inhibitors against BRAF-V600E and MEK may be of clinical relevance (Aylwin et al., 2016; Brastianos et al., 2016). Our mouse models have provided important insights into the molecular pathogenesis of PCP. We reveal the presence of a population of cycling Sox2+ cells in the basal layer surrounding the fibrovascular cores of PCP tumours, suggesting that these cells may be driving tumour growth. Indeed, our analysis shows that most of the cycling cells in the tumour are contained in the Sox2+ve cell compartment. It is interesting that despite the broad expression of the BRAF-V600E mutant

protein in the tumours, pERK1/2 staining is mostly restricted to cells surrounding the fibrovascular cores, a region enriched in Sox2+ve cells. This is very similar to our observations in the mouse models, where the activation of the pathway as evidenced by pERK1/2 staining mostly occurs in the Sox2+ve cells, even if all the pituitary cells express BRAF-V600E. In the human tumours, the squamous epithelium, which is thought to derive from the basal cell layer, does not express any pituitary hormone or cell-lineage commitment marker (PIT1, TPIT and SF1, data not shown), suggesting that as in the mouse, the activation of the MAPK/ERK pathway in human PCP leads to sustained proliferation and impaired differentiation of the Sox2+ve cells. Therefore, although there are differences between human PCP and the mouse models presented here, both have in common that Sox2+ve cells represent the major proliferative cell population and that these show impaired differentiation potential. The perinatal lethality in *Hesx1*$^{Cre/+}$*;Braf*$^{V600E/+}$ mice precluded further analysis and therefore, we cannot conclude whether increased numbers of mutated Sox2+ve cells in the pituitary may eventually drive the formation of PCP-like tumours in these mice at an older age. Further refinement may be required to model PCP more accurately (e.g. using the *Sox2-CreERT2* mouse line (Andoniadou et al). Although hampered by the rarity of these tumours, further research aiming to test whether these cycling Sox2+ve cells may represent a tumour-initiating cell population within human PCP is also warranted.

MATERIALS AND METHODS

Mice

The *Hesx1*$^{Cre/+}$, *Braf*$^{V600E/+}$or *Kras*$^{G12D/+}$ mice have previously been described (Andoniadou et al., 2007; Mercer et al., 2005; Tuveson et al., 2004). In both the *Braf*$^{V600E/+}$ and the *Kras*$^{G12D/+}$ mouse lines the expression of the oncogenic protein is activated upon Cre-mediated recombination. Genotyping of mice and embryos was carried out by PCR on ear punch biopsies or pieces of tissue from embryos digested in DNAreleasy (Anachem) as per manufacturer's instructions. The data presented in this work are representative of examples of at least 3 individual embryos per genotype. All the experiments performed in mice were carried out according to UK Home Office guidance and approved by a local ethical committee.

Histology and *in situ* hybridisation on histological sections

Haematoxylin and Eosin staining was performed as previously described (Gaston-Massuet et al., 2011). Histological processing of embryos and *in situ* hybridisation on paraffin sections was performed as previously described (Gaston-Massuet et al., 2008; Sajedi et al., 2008). The antisense riboprobes used in this study (*Fgf10, Shh, Bmp4, Lhx3*) have been described (Gaston-Massuet et al., 2008; Sajedi et al., 2008; Jayakody et al., 2012; Trowe et al., 2013). Full-length *Braf* and *Kras* antisense riboprobes were obtained from Source Bioscience (Clone ID PX00999A07 and IRAVp968D072D, respectively).

EdU Labeling

For EdU labelling of embryonic pituitaries, pregnant females at 14.5 dpc were subjected to a single intra-peritoneal injection of EdU at a dose of 100mg/kg and embryos dissected either 2 hours later for short term tracing expriments or 48 hours later at 16.5 dpc for longer term tracing. Double immunostaining against specific markers (SOX2, PIT1, TPIT and KI67) and EdU was conducted using the Click-It EdU imaging kit (Invitrogen) according to manufacturer's instructions.

Immunohistochemistry and immunofluorescence

Embryos were fixed in 4% PFA and processed for immunodetection as previously described (Jayakody et al., 2012; Andoniadou et al., 2013). Detection of hormones was carried out using antibodies for α-GH (NHPP AFP-5641801), α-ACTH (10C-CR1096M1), α-TSH (NHPP AFP-1274789), α-PRL (NHPP AFP-425-10-91), α-LH (NHPP AFP-C697071P) and α-FSH (AFP-7798-1289) (Developmental Studies Hybridoma Bank) at a 1:1000 dilution. Detection of pituitary lineage commitment was performed using antibodies for α-PIT1 (Gift from S. Rhodes) and α-TPIT (Gift from J. Drouin) at a 1:1000 dilution. α-SF1 (434200) (Thermo) was used at a dilution of 1:200. Markers of pituitary stem cells α-SOX2 (GT15098, Immune Systems) and α-SOX9 (AB5535, Milipore) were used at a dilution of 1:250 and 1:500, respectively. Proliferation markers α-KI67 (ab16667, Abcam) and α-CYCLIND2 (SC-593, Santa Cruz) were used at a dilution of 1:100 and 1:200, respectively. Detection of activated MAPK signaling cells was performed using α-pERK1/2 (9101, Cell Signaling) at a dilution of 1:250. Cytokeratins were detected using α-pan-cytokeratin recognising cytokeratins 5, 6, 8, 17, 19 (DMNF116; Dako M0821) at a dilution of 1:300, and an antibody specifically recognising cytokeratin 19 (DAKO clone RCK108; no. M088). Detection of

oncogenic BRAF was performed using a α-BRAF V600E antibody (Spring Bioscience; E19290) at a dilution of 1:50.

Cell counting in vivo

All cell counting analysis were performed in 3-5 non-consecutive histological sections immunostained with the specific antibodies. PIT1, SF1, TPIT, KI67, SOX2 and CyclinD2 expressing populations were determined by taking the proportion of positive cells relative to total DAPI positive nuclei. Around 4000 to 7000 DAPI positive cells and 300 to 1000 marker-positive (PIT1+, SF1+, TPIT+, KI67+, SOX2+ and CyclinD2+) cells were counted for each genotype. For analysis of EdU tracing experiments the proportion of either SOX2, PIT1 or KI67 were determined relative to the EdU positive cell population. Around 500 to 1500 EdU positive cells and 200 to 600 marker-positive cells were counted for each genotype. Analysis of hormone producing cell populations (GH+, PRL+, TSH+, FSH+, LH+, ACTH+, αGSU+) was assessed through determining the relative proportion of hormone positive population to total DAPI positive nuclei in a section. These proportions were then applied to average cell counts of dissociated pituitaries to determine an approximation of the absolute numbers of these populations in the pituitary. Around 5500 to 8500 DAPI positive cells and 200 to 2500 marker-positive cells were counted for each genotype.

Assessment of clonogenic potential

Pituitaries from *Hesx1*$^{Cre/+}$; *Braf*$^{V600E/+}$, *Hesx1*$^{Cre/+}$; *Kras*$^{G12D/+}$ and control littermates were dissected at 18.5 dpc and the posterior lobe was removed. Anterior pituitaries were dissociated mechanically into a single cell suspensions following incubation in an enzyme mix (0.5% w/v Collagenase type 2 (Lorne Laboratories Ltd), 0.1X Trypsin (Gibco) and 50 µg/ml DNaseI (Worthington) with 2.5 µg/ml Fungizone (Gibco) in Hank's Balanced Salt

Solution (HBSS (Gibco) for 4 hours at 37°C. Cells were then washed in HBSS, suspended in pituitary stem cell medium and seeded at densities of 2000, 4000 and 8000 cells per well of a 6-well plate for adherent culture. Cells were cultured for 3 days at which point they were fixed with 4% PFA and colonies were stained for haematoxylin, as previously described (Gaston-Massuet et al., 2011). The proportion of colonies observed after 3 days of culture relative to seeded cells was used to estimate total clonogenic cells in 18.5 dpc pituitaries by multiplying this value by the total number of cells quantified following dissociation of the pituitary.

RNA extraction and quantitative real-time PCR

Pituitaries from *Hesx1*$^{Cre/+}$; *Braf*$^{V600E/+}$ or *Hesx1*$^{Cre/+}$; *Kras*$^{G12D/+}$ and control littermates were dissected at 18.5 dpc. The posterior lobe of the pituitary was discarded and the intermediate and anterior lobes were processed for total RNA extraction using the RNeasy Micro kit (Qiagen). Approximately 1 µg of total RNA was reverse transcribed to cDNA using the iScript Reverse Transcription Kit and random hexamers (BIORAD). Quantitative real-time PCR reactions were run in triplicate using the iTaq SYBR Green (BIORAD) and repeated for a minimum of three independent samples for each genotype. Primer sequences are available on request. The absolute number of mRNA copies was determined for each sample by comparison of obtained Cq values with that of a standard of known copy number for each transcript investigated. Variations in input cDNA used for each reaction were accounted for by normalising differences in Gapdh expression between samples and genotypes and applying this normalisation factor to absolute copy numbers obtained for each mRNA species of interest. Primer sequences are available on request.

Human pituitaries and papillary craniopharyngioma samples

Anonymised archival frozen and FFPE specimens of PCP were accessed through Brain UK. Human fetal pituitary tissue was accessed through the Human Developmental Biology Resource (HDBR). Anonymised post mortem human adult pituitary was accessed from the Medical Research Council Edinburgh Brain and Tissue bank and Royal Victoria Infirmary, Newcastle, UK (Ethical approval

14/LO/2265).

Detection of BRAF p.V600E mutations in papillary craniopharyngioma tumours

DNA was diluted 5-fold with nuclease-free water (Ambion). Each digital PCR reaction was made up to 20 µL with 2 µL diluted DNA, 10 µL ddPCR™ Supermix for Probes (No dUTP; Bio-Rad), forward & reverse primers, dual-labelled probes for wild-type and mutant templates, and nuclease-free water. Sequences for the BRAF-V600E assay oligonucleotides are from Hindson et al. (2011) and were used at the concentrations stated. Reactions were partitioned into ~23,000 droplets with Droplet Generation Oil for Probes (Bio-Rad) using the QX200 Droplet Generator (Bio-Rad). All samples were tested in duplicate, with no-template controls included in all columns. Standard cycling conditions as recommended by the manufacturer were used with a T_a of 60°C. Results were analysed with QuantaSoft ™ software, v1.7. A mean of 19,080 droplets were successfully read in each well, including controls. Two droplets positive for wild-type template were seen in the negative controls, indicating a negligible degree of contamination.

Statistics

Mendelian ratios were evaluated using the chi-squared test. Clonogenic potential of control, *Hesx1*$^{Cre/+}$;*Kras*$^{G12D/+}$ and *Hesx1*$^{Cre/+}$;*Braf*$^{V600E/+}$ pituitaries was evaluated using a paired t-test. Total cell counts of control and mutant pituitaries and quantitative real-time PCR data were analysed by unpaired t-test.

ACKNOWLEDGMENTS

We thank the Developmental Studies Hybridoma Bank (University of Iowa) and the National Hormone and Peptide Program (Harbor–University of California, Los Angeles Medical Center) for providing some of the antibodies used in this study. The human embryonic and fetal material was provided by the Joint Medical Research Council (MRC)/Wellcome Trust Human Developmental Biology Resource (www.hdbr.org) (Grant 099175/Z/12/Z). PCP tissue samples were also obtained from Plymouth Hospitals NHS Trust as part of the UK Brain Archive Information Network (BRAIN UK), which is funded by the Medical Research Council and braintrust. Adult pituitary tissue was obtained from the Medical Research Council Edinburgh Brain and Tissue Bank and from Dr Abhijit Joshi (Royal Victoria Infirmary, Newcastle, UK). This work was supported by the Medical Research Council (MRC) (Grants MR/M000125/1 and MR/L016729/1) and by the National Institute for Health Research Biomedical Research Centre at Great Ormond Street Hospital for Children National Health Service Foundation Trust and University College London. J.R.A. is a Cancer Research UK Clinical Research Training Fellow. S.H. holds a Wellcome Trust PhD Fellowship. J.P.M.-B. is a Great Ormond Street Children Hospital Charity Principal Investigator.

COMPETING INTERESTS

T.F. is a co-founder, shareholder and manager of Inivata. Inivata is a company focused on developing assays for circulating tumour DNA analysis. All the other authors declare no competing interests.

AUTHOR CONTRIBUTIONS

S.H. carried out the majority of the experiments and contributed to experimental design. S.P., G.C and J.M.P.-M. performed the *in situ* hybridisation on embryos and qRT-PCR. S.M. analysed the lung defects. L.P carried out all the genotyping experiments. A.V. and J.A identified the PCP samples and performed sectioning and immunohistochemistry. T.J., S.T. and S.B. contributed to the histopathological assessment. A.G and T. F performed the DNA sequencing of PCP tumours. R.M. provided the Braf-V600E mouse model. C.L.A. contributed to experimental design and interpretation. J.P.M.-B. designed the experiments and overviewed the project. J.P.M.-B. and S.H. wrote the paper.

FUNDING

Medical Research Council (MRC) (Grants MR/M000125/1 and MR/L016729/1)

National Institute for Health Research Biomedical Research Centre at Great Ormond Street Hospital for Children National Health Service Foundation Trust and University College London.

Wellcome Trust (PhD Fellowship).

Cancer Research UK (PhD Fellowship).

REFERENCES

Andoniadou, C. L., Matsushima, D., Mousavy Gharavy, S. N., Signore, M., Mackintosh, A. I., Schaeffer, M., Gaston-Massuet, C., Mollard, P., Jacques, T. S., Le Tissier, P. et al. (2013) 'Sox2(+) stem/progenitor cells in the adult mouse pituitary support organ homeostasis and have tumor-inducing potential', *Cell Stem Cell* **13** (4): 433-45.

Andoniadou, C. L., Signore, M., Sajedi, E., Gaston-Massuet, C., Kelberman, D., Burns, A. J., Itasaki, N., Dattani, M. and Martinez-Barbera, J. P. (2007) 'Lack of the murine homeobox gene Hesx1 leads to a posterior transformation of the anterior forebrain', *Development* **134** (8): 1499-508.

Aylwin, S. J., Bodi, I. and Beaney, R. (2016) 'Pronounced response of papillary craniopharyngioma to treatment with vemurafenib, a BRAF inhibitor', *Pituitary* **19** (5): 544-6.

Bilodeau, S., Roussel-Gervais, A. and Drouin, J. (2009) 'Distinct developmental roles of cell cycle inhibitors p57Kip2 and p27Kip1 distinguish pituitary progenitor cell cycle exit from cell cycle reentry of differentiated cells', *Molecular and Cellular Biology* **29** (7): 1895-908.

Booth, A., Trudeau, T., Gomez, C., Lucia, M.S., Gutierrez-Hartmann, A. (2014) 'Persistent ERK/MAPK activation promotes lactotrope differentiation and diminishes tumorigenic phenotype', *Molecular Endocrinology* **28** (12): 1999-2011.

Brastianos, P. K., Shankar, G. M., Gill, C. M., Taylor-Weiner, A., Nayyar, N., Panka, D. J., Sullivan, R. J., Frederick, D. T., Abedalthagafi, M., Jones, P. S. et al. (2016) 'Dramatic Response of BRAF V600E Mutant Papillary Craniopharyngioma to Targeted Therapy', *Journal of the National Cancer Institute* **108** (2).

Brastianos, P. K., Taylor-Weiner, A., Manley, P. E., Jones, R. T., Dias-Santagata, D., Thorner, A. R., Lawrence, M. S., Rodriguez, F. J., Bernardo, L. A., Schubert, L. et al. (2014) 'Exome sequencing identifies BRAF mutations in papillary craniopharyngiomas', *Nature Genetics* **46** (2): 161-5.

Castinetti, F., Davis, S. W., Brue, T. and Camper, S. A. (2011) 'Pituitary stem cell update and potential implications for treating hypopituitarism', *Endocrine Reviews* **32** (4): 453-71.

Davis, S.W., Mortensen A.H., Camper S.A. (2011) 'Birthdating studies reshape models for pituitary glad specification', *Developmental Biology* **352** (2): 215-27.

De Moerlooze, L., Spencer-Dene, B., Revest, J. M., Hajihosseini, M., Rosewell, I. and Dickson, C. (2000) 'An important role for the IIIb isoform of fibroblast growth factor receptor 2 (FGFR2) in mesenchymal-epithelial signalling during mouse organogenesis', *Development* **127** (3): 483-92.

Dhillon, A. S., Hagan, S., Rath, O. and Kolch, W. (2007) 'MAP kinase signalling pathways in cancer', *Oncogene* **26** (22): 3279-90.

Dolle, P., Castrillo, J. L., Theill, L. E., Deerinck, T., Ellisman, M. and Karin, M. (1990) 'Expression of GHF-1 protein in mouse pituitaries correlates both temporally and spatially with the onset of growth hormone gene activity', *Cell* **60** (5): 809-20.

Dworakowska, D., Wlodek, E., Leontiou, C. A., Igreja, S., Cakir, M., Teng, M., Prodromou, N., Goth, M. I., Grozinsky-Glasberg, S., Gueorguiev, M. et al. (2009) 'Activation of RAF/MEK/ERK and PI3K/AKT/mTOR pathways in pituitary adenomas and their effects on downstream effectors', *Endocr Relat Cancer* **16** (4): 1329-38.

Ericson, J., Norlin, S., Jessell, T. M. and Edlund, T. (1998) 'Integrated FGF and BMP signaling controls the progression of progenitor cell differentiation and the emergence of pattern in the embryonic anterior pituitary', *Development* **125** (6): 1005-15.

Ewing, I., Pedder-Smith, S., Franchi, G., Ruscica, M., Emery, M., Vax, V., Garcia, E., Czirjak, S., Hanzely, Z., Kola, B., Korbonits, M., Grossman, A.B. (2007) 'A mutation and expression analysis of the oncogene BRAF in pituitary adenomas', *Clinical Endocrinology (Oxf)*. **66** (3): 348-352.

Fang, Q., George, A. S., Brinkmeier, M. L., Mortensen, A. H., Gergics, P., Cheung, L. Y., Daly, A. Z., Ajmal, A., Perez Millan, M. I., Ozel, A. B. et al. (2016) 'Genetics of Combined Pituitary Hormone Deficiency: Roadmap into the Genome Era', *Endocrine Reviews* **37** (6): 636-675.

Fauquier, T., Rizzoti, K., Dattani, M., Lovell-Badge, R. and Robinson, I. C. (2008) 'SOX2-expressing progenitor cells generate all of the major cell types in the adult mouse pituitary gland', *Proceedings of the National Academy of Sciences of the United States of America* **105** (8): 2907-12.

Garcia-Lavandeira, M., Quereda, V., Flores, I., Saez, C., Diaz-Rodrigues, E., Japon, M.A., Ryan, A.K., Blasco, M.A., Dieguez, C., Malumbres, M., Alvarez, C.Z. (2009) 'A GRFa2/Prop1/stem (GPS) cell niche in the pituitary', *PLoS One* **4** (3): e4815

Gaston-Massuet, C., Andoniadou, C. L., Signore, M., Jayakody, S. A., Charolidi, N., Kyeyune, R., Vernay, B., Jacques, T. S., Taketo, M. M., Le Tissier, P. et al. (2011) 'Increased Wingless (Wnt) signaling in pituitary progenitor/stem cells gives rise to pituitary tumors in mice and humans', *Proceedings of the National Academy of Sciences of the United States of America* **108** (28): 11482-7.

Gaston-Massuet, C., Andoniadou, C. L., Signore, M., Sajedi, E., Bird, S., Turner, J. M. and Martinez-Barbera, J. P. (2008) 'Genetic interaction between the homeobox transcription factors HESX1 and SIX3 is required for normal pituitary development', *Developmental Biology* **324** (2): 322-33.

Goldsmith, S., Lovell-Badge, R., Rizzoti, K. (2016) 'SOX2 is sequentially required for progenitor proliferation and lineage specification in the developing pituitary', *Development* **143** (13) 2376-88.

Hindson, B. J., Ness, K. D., Masquelier, D. A., Belgrader, P., Heredia, N. J., Makarewicz, A. J., Bright, I. J., Lucero, M. Y., Hiddensen, A. L., Legler, T. C., et al. (2011). High-throughput droplet digital PCR system for absolute quantitation of DNA copy number. *Analytical chemistry*, **83** (22), 8604-8610.

Jayakody, S. A., Andoniadou, C. L., Gaston-Massuet, C., Signore, M., Cariboni, A., Bouloux, P. M., Le Tissier, P., Pevny, L. H., Dattani, M. T. and Martinez-Barbera, J. P. (2012) 'SOX2 regulates the hypothalamic-pituitary axis at multiple levels', *Journal of Clinical Investigation* **122** (10): 3635-46.

Karga, H.J., Alexander, J.M., Hedley-Whyte, E.T., Klibanski, A., Jameson, J.L. (1992) 'Ras mutations in human pituitary tumors', *The Journal of Clinical Endocrinology & Metabolsm* **74** (4): 914-919.

Kelberman, D., Rizzoti, K., Lovell-Badge, R., Robinson, I. C. and Dattani, M. T. (2009) 'Genetic regulation of pituitary gland development in human and mouse', *Endocrine Reviews* **30** (7): 790-829.

Lamolet, B., Pulichino, A. M., Lamonerie, T., Gauthier, Y., Brue, T., Enjalbert, A. **and Drouin, J.** (2001) 'A pituitary cell-restricted T box factor, Tpit, activates POMC transcription in cooperation with Pitx homeoproteins', *Cell* **104** (6): 849-59.

Louis DN, Ohgaki H, Wiestler OD and WK, C. (2016) WHO Classification of Tumours of the Central Nervous System *WHO/IARC Classification of Tumours*, vol. Volume 1.

Mercer, K., Giblett, S., Green, S., Lloyd, D., DaRocha Dias, S., Plumb, M., Marais, R., Pritchard, C. (2005) 'Expression of endogenous oncogenic V600E B-raf induces

proliferation and developmental defects in mice and transformation of primary fibroblasts', *Cancer Research* **65** (24): 11493-11500.

Mollard, P., Hodson, D. J., Lafont, C., Rizzoti, K. and Drouin, J. (2012) 'A tridimensional view of pituitary development and function', *Trends Endocrinol Metab* **23** (6): 261-9.

Newey, P.J., Nesbit, M.A., Rimmer, A.J., Head, R.A., Gorvin, C.M., Attar, M., Gregory, L., Wass, J.A., Buck, D., Karavitaki, N., Grossman, A.B., McVean, G., Ansorge, O., Thakker, R.V. (2013) 'Whole-exome sequencing studies of nonfunctioning pituitary adenomas' *Journal of Clinical Endocrinology & Metabolism*. **98** (4): E796-800.

Norlin, S., Nordstrom, U. and Edlund, T. (2000) 'Fibroblast growth factor signaling is required for the proliferation and patterning of progenitor cells in the developing anterior pituitary', *Mechanisms of Development* **96** (2): 175-82.

Ohuchi, H., Hori, Y., Yamasaki, M., Harada, H., Sekine, K., Kato, S. and Itoh, N. (2000) 'FGF10 acts as a major ligand for FGF receptor 2 IIIb in mouse multi-organ development', *Biochemical and Biophysical Research Communications* **277** (3): 643-9.

Ornitz, D. M. and Itoh, N. (2015) 'The Fibroblast Growth Factor signaling pathway', *Wiley Interdiscip Rev Dev Biol* **4** (3): 215-66.

Pérez Millán, M.I., Brinkmeier, M.L., Mortensen, A.H., Camper, S.A. (2016) 'PROP-1 triggers epithelial-mesenchymal transition-like proces in pituitary stem cells', *Elife* **5** e14470.

Reincke, M., Sbiera, S., Hayakawa, A., Theodoropoulou, M., Osswald, A., Beuschlein, F., Meitinger, T., Mizuno-Yamasaki, E., Kawaguchi, K., Saeki, Y., Tanaka, K., Wieland, T., Graf, E., Saeger, W., Ronchi, C.L., Allolio, B., Buchfelder, M., Strom, T.M., Fassnacht, M., Komada, M. (2015) 'Mutations in the deubiquitinase gene USP8 cause Cushing's disease' *Nature Genetics* **47** (1): 31-38.

Rizzoti, K., Akiyama, H. and Lovell-Badge, R. (2013) 'Mobilized adult pituitary stem cells contribute to endocrine regeneration in response to physiological demand', *Cell Stem Cell* **13** (4): 419-32.

Ronchi, C.L., Peverelli, E., Herterich, S., Weigand, I., Mantovani, G., Schwarzmayr, T., Sbiera, S., Allolio, B., Honegger, J., Appenzeller, S., Lania, A.G., Reincke, M., Calebiro, D., Spada, A., Buchfelder, M., Flitsch, J., Strom, T.M., Fassnacht, M. (2016) 'Landscape of somatic mutations in sporadic GH-secreting pituitary adenomas' *European Journal of Endocrinology* **174** (3): 363-372.

Sajedi, E., Gaston-Massuet, C., Signore, M., Andoniadou, C. L., Kelberman, D., Castro, S., Etchevers, H. C., Gerrelli, D., Dattani, M. T. and Martinez-Barbera, J. P. (2008) 'Analysis of mouse models carrying the I26T and R160C substitutions in the transcriptional repressor HESX1 as models for septo-optic dysplasia and hypopituitarism', *Dis Model Mech* **1** (4-5): 241-54.

Schimmer, B. P. and White, P. C. (2010) 'Minireview: steroidogenic factor 1: its roles in differentiation, development, and disease', *Molecular Endocrinology* **24** (7): 1322-37.

Tang, N., Marshall, W. F., McMahon, M., Metzger, R. J. and Martin, G. R. (2011) 'Control of mitotic spindle angle by the RAS-regulated ERK1/2 pathway determines lung tube shape', *Science* **333** (6040): 342-5.

Treier, M., Gleiberman, A. S., O'Connell, S. M., Szeto, D. P., McMahon, J. A., McMahon, A. P. and Rosenfeld, M. G. (1998) 'Multistep signaling requirements for pituitary organogenesis in vivo', *Genes Dev* **12** (11): 1691-704.

Treier, M., O'Connell, S., Gleiberman, A., Price, J., Szeto, D. P., Burgess, R., Chuang, P. T., McMahon, A. P. and Rosenfeld, M. G. (2001) 'Hedgehog signaling is required for pituitary gland development', *Development* **128** (3): 377-86.

Trowe, M. O., Zhao, L., Weiss, A. C., Christoffels, V., Epstein, D. J. and Kispert, A. (2013) 'Inhibition of Sox2-dependent activation of Shh in the ventral diencephalon by Tbx3 is required for formation of the neurohypophysis', *Development* **140** (11): 2299-309.

Tuveson, D.A., Shaw, A.T., Willis, N.A., Silver, D.P., Jackson, E.L., Chang, S., Mercer, K.L., Grochow, R., Hock, H., Crowley, D., Hingorani, S.R., Zaks, T., King, C., Jacobetz, M.A., Wang, L., Bronson, R.T., Orkin, S.H., DePinho, R.A., Jacks, T. (2004) 'Endogenous oncogenic K-ras(G12D) stimulates proliferation and widespread neoplastic and developmental defects' *Cancer Cell* **5** (4): 375-387.

Välimäki, N., Demir, H., Pitkanen, E., Kaasinen, E., Karppinen, A., Kivipelto, L., Schalin-Jantti, C., Aaltonen, L.A., Karhu, A. (2015) 'Whole-Genome Sequencing of Growth Hormone (GH)-Secreting Pituitary Adenomas' *Journal of Clinical Endocrinology & Metabolism* **100** (10) 3918-3927.

Zhang, W. and Liu, H. T. (2002) 'MAPK signal pathways in the regulation of cell proliferation in mammalian cells', *Cell Research* **12** (1): 9-18.

Figures

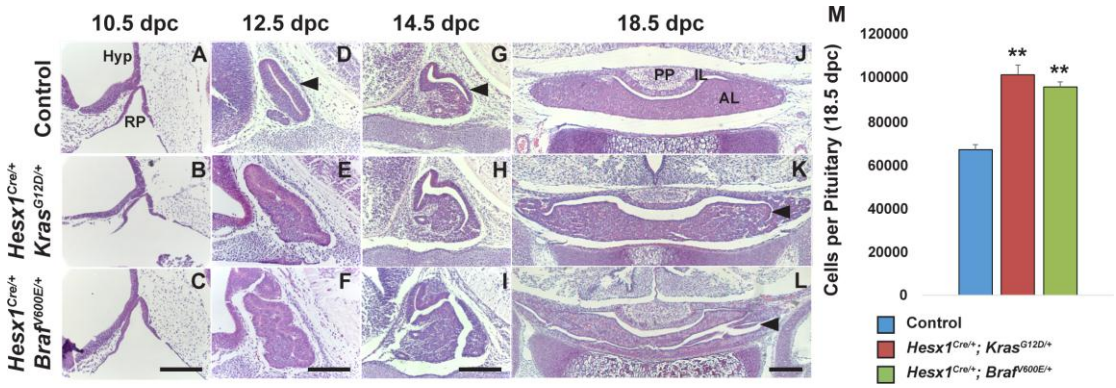

Figure 1. Abnormal pituitary morphogenesis in *Hesx1*$^{Cre/+}$;*Kras*$^{G12D/+}$ and *Hesx1*$^{Cre/+}$;*Braf*$^{V600E/+}$ mutants. Hematoxylin and eosin staining of sagittal (A-I) or transverse (J-L) histological sections of the developing pituitary gland in control and mutant embryos; genotypes and stages are indicated. **(A-C)** At 10.5 dpc, Rathke's pouch (RP) is morphologically comparable between genotypes. **(D-I)** The developing pituitary is enlarged and dysmorphic in the mutant compared with the control pituitary at 12.5 and 14.5 dpc (arrowheads). **(J-L)** At 18.5 dpc, the cleft is expanded and ramified in the mutant pituitaries (arrowheads in K,L) compared with the control (J). The posterior pituitary (PP) is comparable between genotypes. **(M)** Quantification of total numbers of cells in the control, *Hesx1*$^{Cre/+}$;*Kras*$^{G12D/+}$ and *Hesx1*$^{Cre/+}$;*Braf*$^{V600E/+}$ pituitaries at 18.5 dpc showing a significant increase in the mutants. Scale bar is 200 μm.

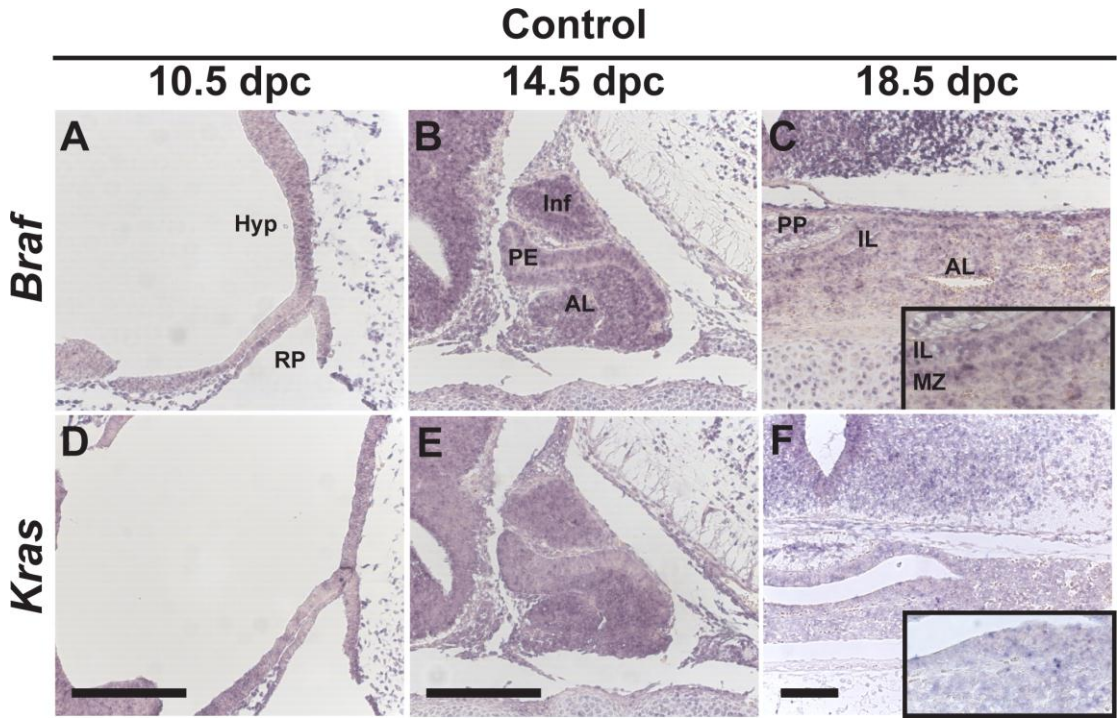

Figure 2. *Braf* and *Kras* mRNA is detected in the developing hypothalamus and pituitary gland. *In situ* hybridisation using *Braf* and *Kras* antisense riboprobes on histological sections of developing wild-type pituitaries. **(A,D)** At 10.5 dpc, weak over-all expression of *Braf* and *Kras* is detected in the prospective hypothalamus (Hyp) and Rathke's pouch (RP). **(B,E)** At 12.5 dpc, strong expression is detected in the infundibulum (Inf), hypothalamus (Hyp), periluminal epithelium (PE) and developing anterior lobe (AL). **(C,F)** At 18.5 dpc, expression is detected in specific cells within the posterior pituitary (PP), intermediate lobe (IL) and the parenchyma of the anterior lobe (AL) including the marginal zone (MZ). Scale bar is 200μm.

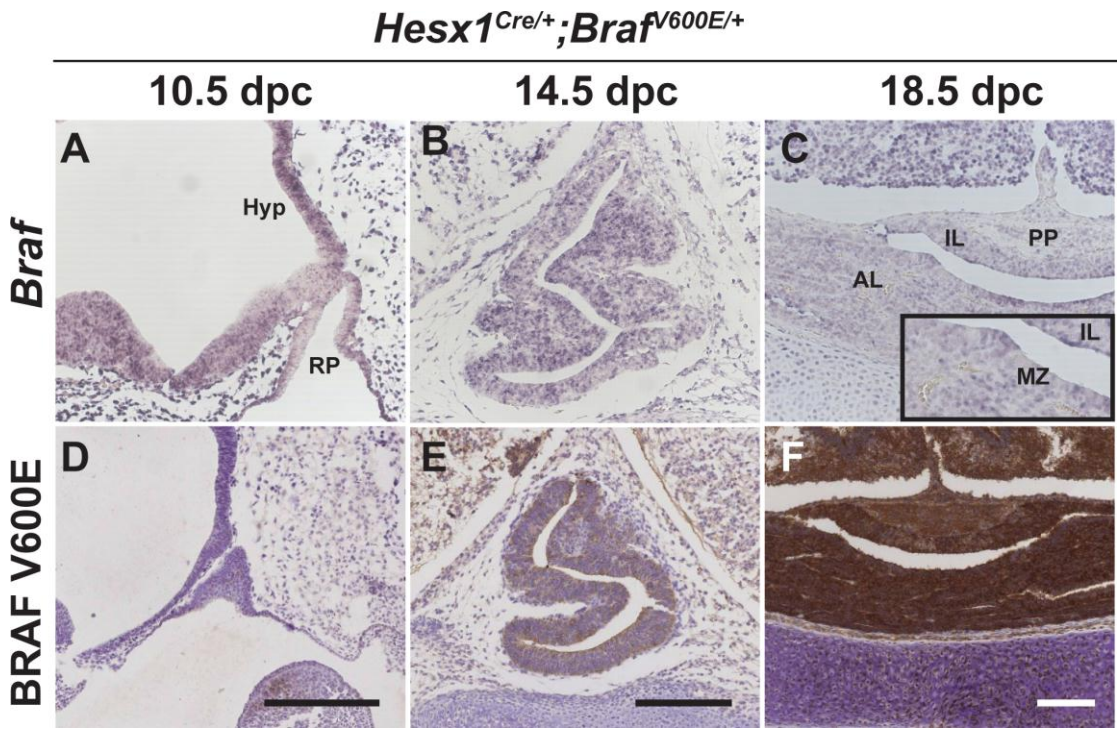

Figure 3. *Braf* mRNA and BRAF-V600E protein are expressed in the developing pituitary in *Hesx1*$^{Cre/+}$;*Braf*$^{V600E/+}$ mutants. *In situ* hybridisation using *Braf* antisense riboprobes (A-C) and immunohistochemistry against BRAF-V600E mutant protein (D-F) on histological sections of *Hesx1*$^{Cre/+}$;*Braf*$^{V600E/+}$ embryos at indicated stages. **(A-C)** *Braf* mRNA expression is detected in the hypothalamic neuroepithelium (Hyp) and developing pituitary at all stages analysed with a similar expression pattern to the wild-type embryos (Fig. 2A-C). **(D-F)** At 10.5 dpc, only a few cells express the BRAF-V600E protein in the developing Rathke's pouch (RP), but numbers increased from 12.5-18.5 dpc . Scale bar is 200μm.

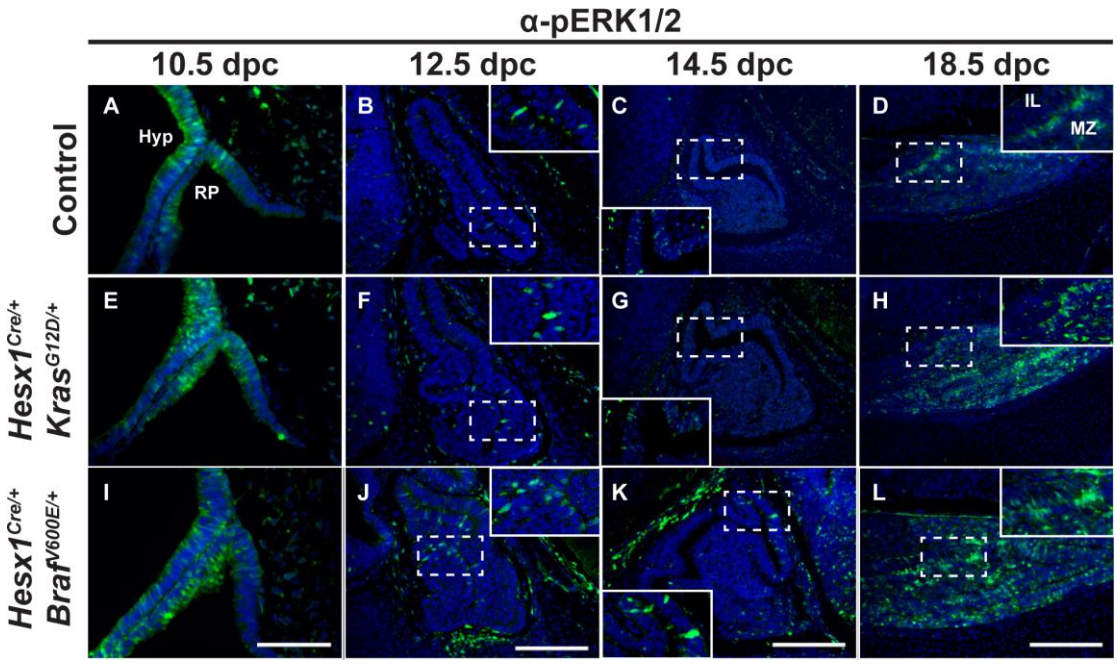

Figure 4. Temporal and spatial regulation of pERK1/2 expression developing pituitary. Immunofluorescent staining against pERK1/2 on histological sections of control and mutant pituitaries; genotypes and stages are indicated. **(A-D)** Abundant pERK1/2+ve cells are detected in the hypothalamus (Hyp) and Rathke's pouch (RP) at 10.5 dpc, but only very few cells express pERK1/2 at 12.5 and 14.5 dpc. At 18.5 dpc, most of the signal is restricted to the intermediate lobe (IL) and marginal zone (MZ) of the anterior lobe. **(E-L)** A similar expression pattern is observed in both *Hesx1*$^{Cre/+}$;*Kras*$^{G12D/+}$ (E-H) and *Hesx1*$^{Cre/+}$;*Braf*$^{V600E/+}$ (I-L) mutant pituitaries. However, the pERK1/2 signal is markedly increased at 18.5 dpc pituitaries (H,L) relative to the control (D). Scale bar is 200μm.

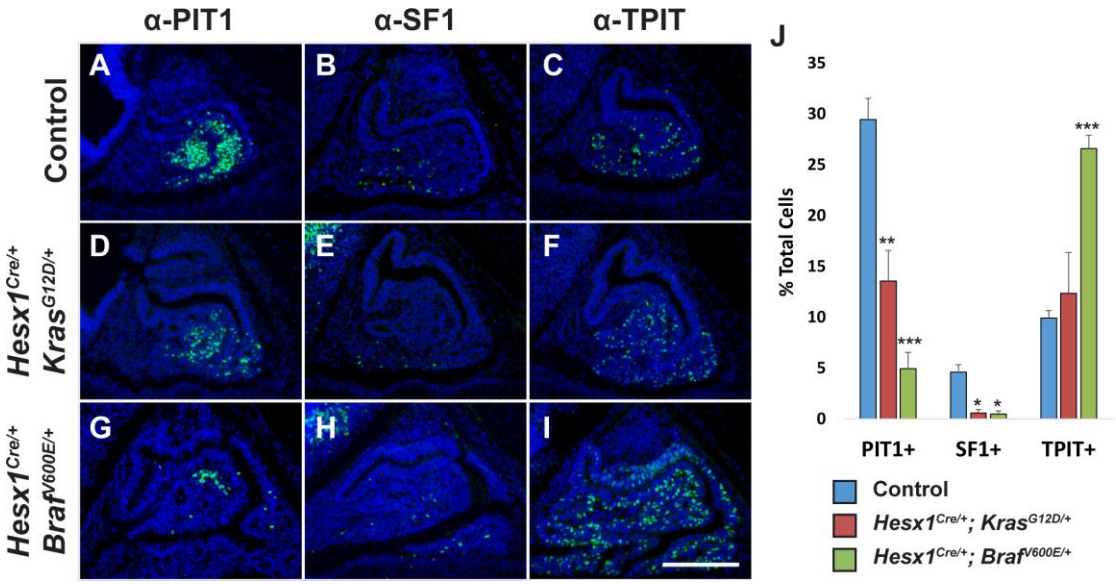

Figure 5. Cell-lineage commitment is disrupted in *Hesx1*$^{Cre/+}$;*Kras*$^{G12D/+}$ and *Hesx1*$^{Cre/+}$;*Braf*$^{V600E/+}$ mutants. Immunostaining against the commitment markers PIT1, SF1 and TPIT on sagittal histological sections of mutant and control embryos at 14.5 dpc. **(A-I)** The expression of TPIT (A,D,G) and SF1 (B,E,H) are markedly reduced in the mutant pituitary, specially in the *Hesx1*$^{Cre/+}$;*Braf*$^{V600E/+}$ mutant, relative to the control. In contrast, TPIT expression is elevated in the mutant pituitary, more apparently in the *Hesx1*$^{Cre/+}$;*Braf*$^{V600E/+}$ genotype (C,F,I). **(J)** Quantification analyses demonstrate the significant reduction of PIT1+ve and SF1+ve cells in both mutants relative to the control pituitary, but the increase of TPIT+ve cells is significant only in the *Braf* mutants. Scale bar is 200μm.

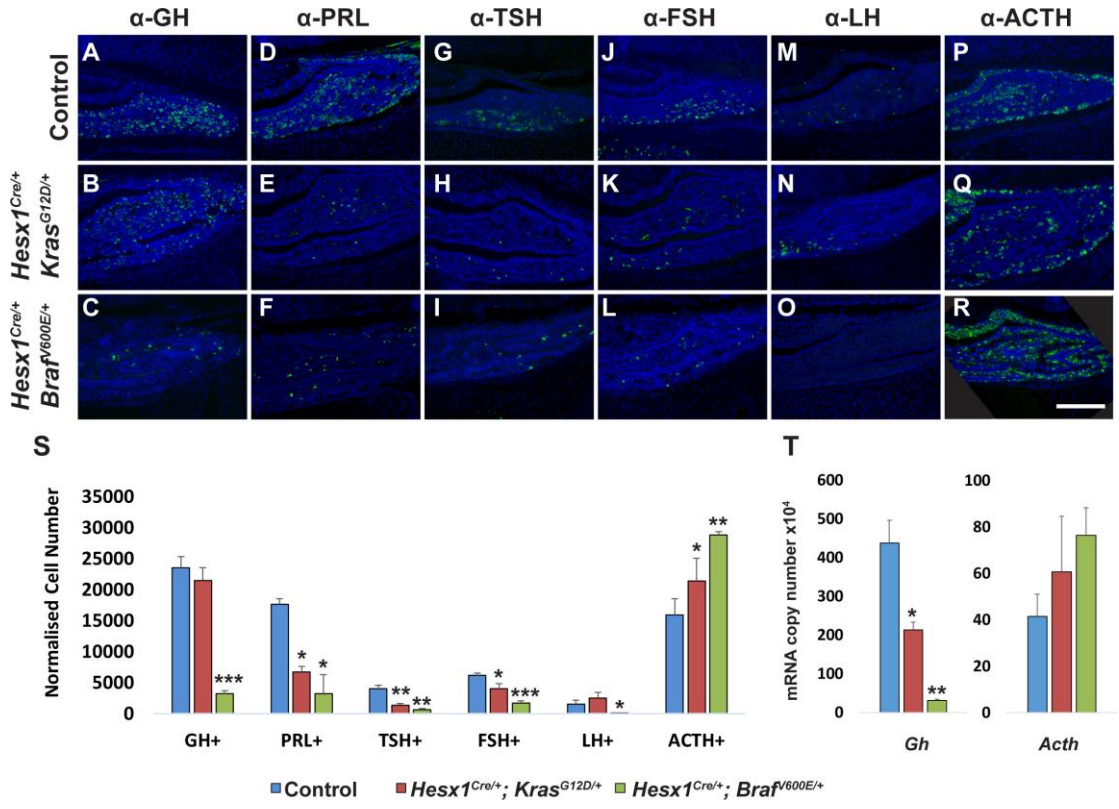

Figure 6. Terminal differentiation of hormone-producing cells is impaired in *Hesx1*$^{Cre/+}$*;Kras*$^{G12D/+}$ and *Hesx1*$^{Cre/+}$*;Braf*$^{V600E/+}$ mutants. Immunostaining against pituitary hormones on transverse histological sections of mutant and control embryos at 18.5 dpc. **(A-R)** Numbers of GH+ve (somatotrophs) (A-C), PRL+ve (lactotrophs) (D-F), TSH+ve (thyrotrophs) (G-I), as well as FSH+ve and LH+ve (gonadotrophs) cells (J-O) appear reduced in the *braf* and *Kras* mutants relative to the control pituitary. (P-R) ACTH+ve cells (corticotrophs and melanotrophs) look increased in the mutant pituitaries compared with the control. **(S)** Quantitative analyses demonstrate a significant reduction of all of the hormone-producing cells in the *Hesx1*$^{Cre/+}$*;Braf*$^{V600E/+}$ mutant pituitary, except for ACTH+ve cells, which are markedly increased relative to controls. *Hesx1*$^{Cre/+}$*;Kras*$^{G12D/+}$ mutant pituitaries show a significant decrease of only PRL+ve, TSH+ve and FSH+ve cells, and ACTH+ve are also increased. **(T)** Absolute quantitative RT-PCR analysis of *Gh* and *Acth* mRNA expression

in mutant and control pituitaries at 18.5dpc. Significance is only reached for *Gh* expression, but there is a trend towards an increase in *Acth* expression. Scale bar is 200μm.

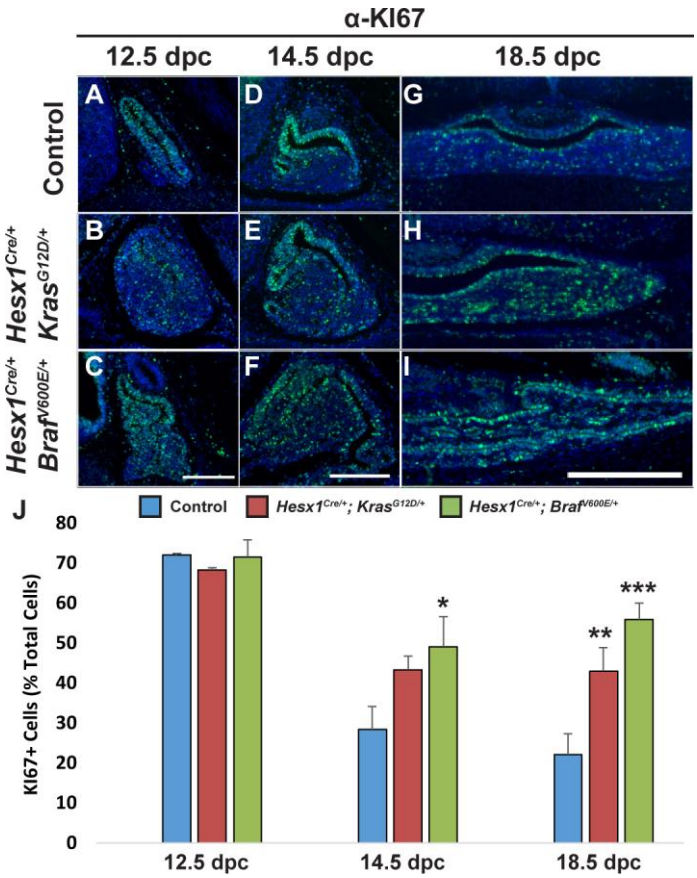

Fig. 7. Increased proliferation in the *Hesx1*$^{Cre/+}$;*Kras*$^{G12D/+}$ and *Hesx1*$^{Cre/+}$;*Braf*$^{V600E/+}$ mutant pituitaries. (A-I) Immunofluorescent staining against Ki67 on histological sections of mutant and control embryos; genotypes and stages are indicated. **(J)** Quantitative analyses of Ki67+ve cells out of the total DAPI+ cells demonstrate a significant increase of the proliferation index in the *Hesx1*$^{Cre/+}$;*Kras*$^{G12D/+}$ at 18.5 dpc and *Hesx1*$^{Cre/+}$;*Braf*$^{V600E/+}$ at 14.5 and 18.5 dpc. Scale bar is 200μm.

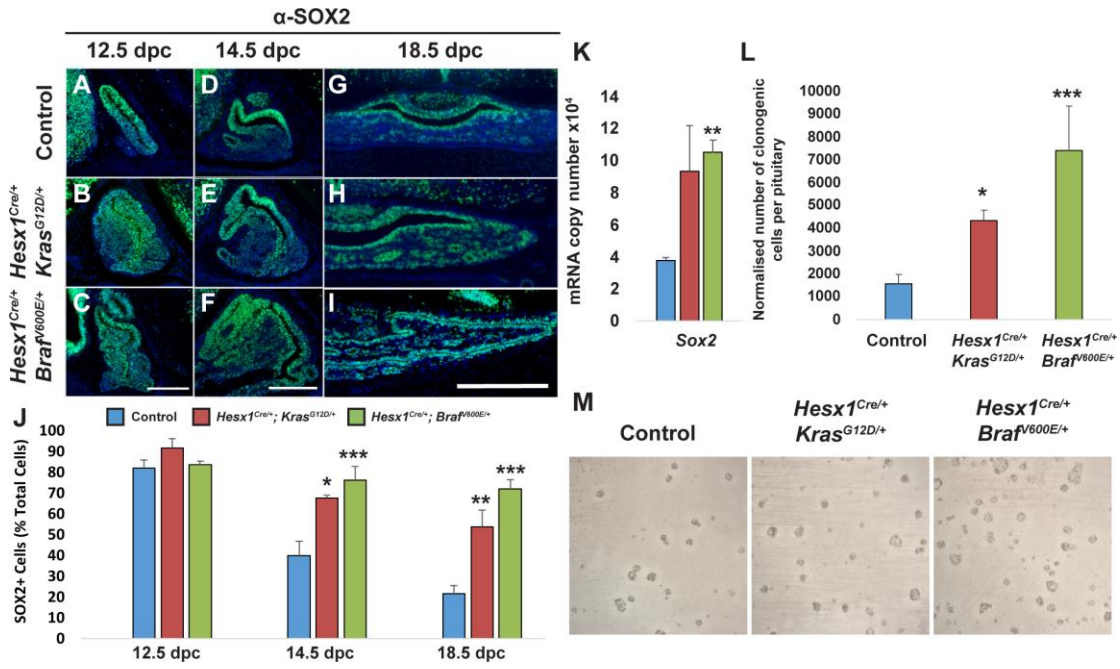

Fig. 8. The Sox2+ve stem cell compartment is increased in *Hesx1*$^{Cre/+}$;*Kras*$^{G12D/+}$ and *Hesx1*$^{Cre/+}$;*Braf*$^{V600E/+}$ mutant pituitaries. (A-I) Immunofluorescence staining revealing the presence of SOX2+ve cells in the developing pituitary; genotypes and stages are indicated. Note that the overall numbers appear elevated in the mutant pituitary relative to the controls at all stages analysed. **(J)** Quantitative analyses demonstrate that SOX2+ve cells are significantly increased in the mutant pituitaries compared to controls at 14.5 and 18.5 dpc. **(K)** Absolute quantitative RT-PCR analysis of *Sox2* mRNA expression in mutant and control pituitaries at 18.5dpc. **(L,M)** Culture of dissociated cells reveals a significant higher clonogenic potential of the mutant pituitaries relative to the controls. Scale bar is 200μm.

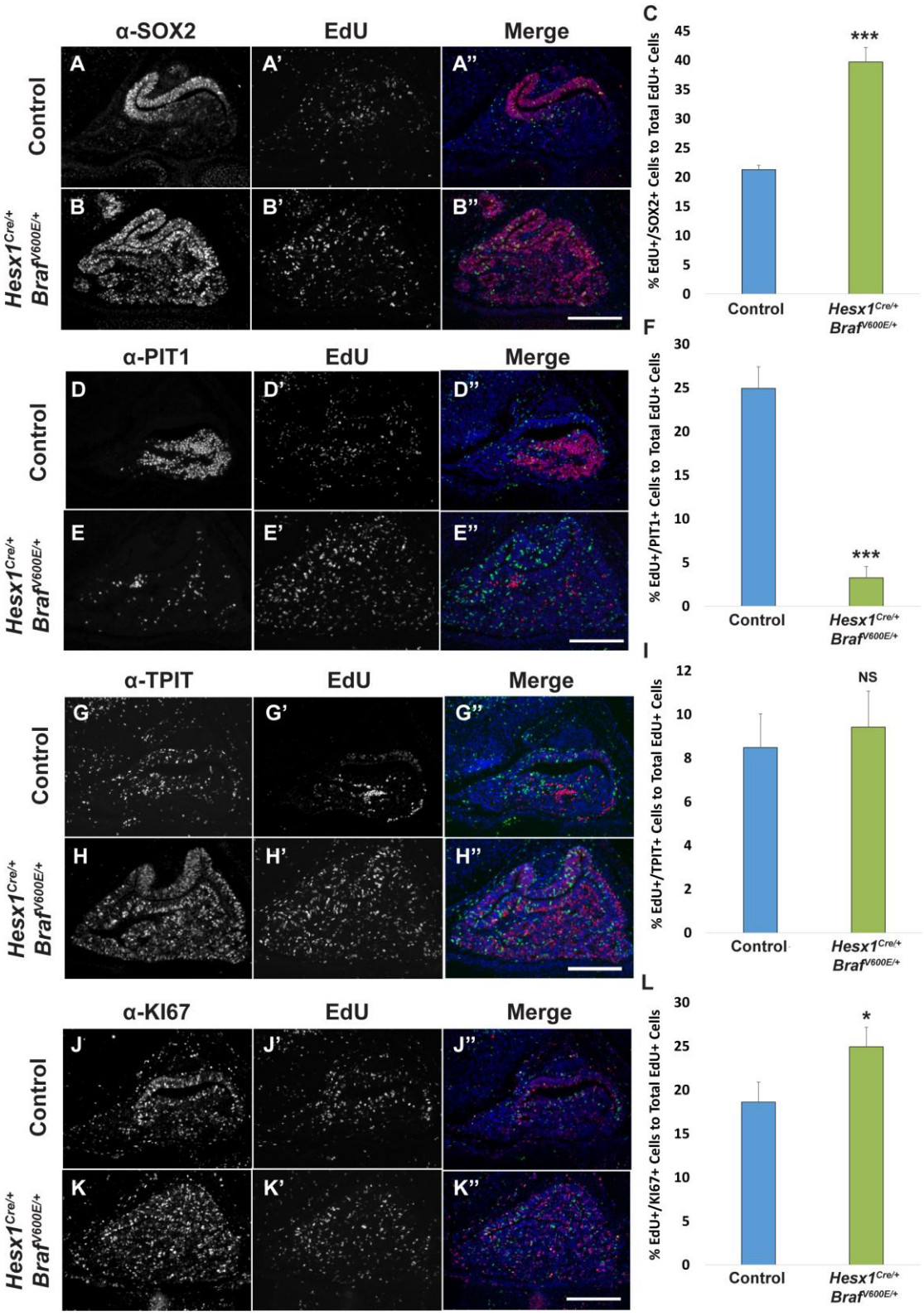

Fig. 9. Abnormal balance between self-renewal and differentiation in the *Hesx1*$^{Cre/+}$*;Braf*$^{V600E/+}$ mutant pituitaries. The nucleotide analogue EdU was administered once to pregnant females at 14.5 dpc and embryos analysed at 16.5 dpc. (**A-C**) Numbers of SOX2;EDU double positive cells in increased in the mutant pituitary relative to the control. **(D-F)** In contrast, the proportion of PIT1;EDU double positive cells is dramatically reduced in the mutant gland. **(G-I)** The proportion of TPIT;EDU double positive cells remained constant between genotypes. **(J-L)** The percentage of cycling cells within the initially EdU-labelled population is significantly higher in the *Hesx1*$^{Cre/+}$*;Braf*$^{V600E/+}$ mutants compared to controls. Scale bar is 200μm.

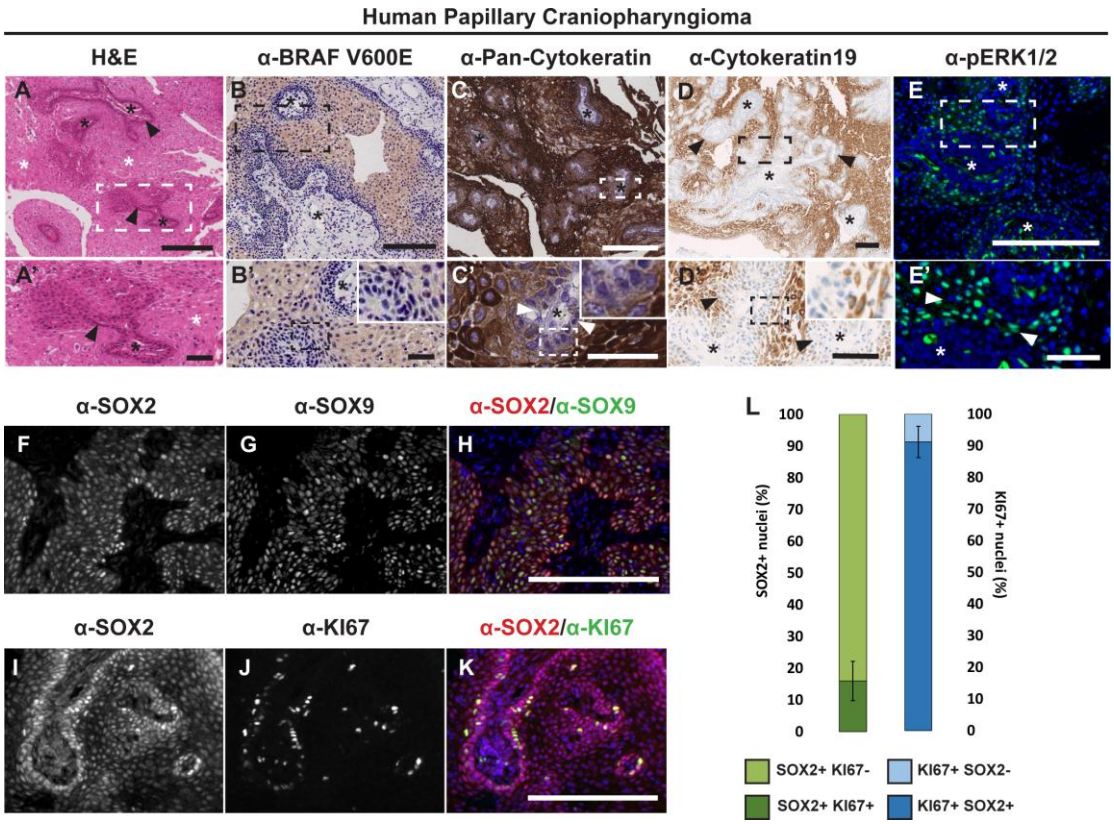

Fig. 10. Human PCP tumours contain a population of cycling SOX2+ve cells. Analysis of histological sections of human PCP tumours. **(A, A')** Hematoxylin eosin staining showing the presence of fibrovascular cores (black asterisks) lined by a layer of basal cells (arrowheads) and large areas of suprabasal squamous epithelium (white asterisk). **(B,B')** Immunohistochemistry revealing the expression of BRAF-V600E in a PCP tumour. Note the presence of staining (light brown) in the vast majority of tumour cells. Black asterisks show the presence of fibrovascular cores. **(C,C')** Immunohistochemical detection using a pan-cytokeratin antibody. Note that most of the tumour cells show positive staining (dark brown) with the exception of the basal cell layer (arrowheads) surrounding the fibrovascular cores (black asterisk). **(D,D')** Specific staining (light brown) against cytokeratin 19 showing absent staining in the basal layer cells. The difference in the staining, from light to dark brown, is a due to technical reasons (e.g. antibody used, manual or automatized immunohistochemistry)

(E,E') Immunofluorescence staining of pERK1/2 showing expression restricted to the cells surrounding the fibrovascular cores (white arrowheads), with some positive cells within the fibrovascular cores (white asterisk). **(F-H)** Double immunofluorescent staining shows the co-expression of SOX2 and SOX9 in cells surrounding the fibrovascular cores, with stronger signal in the basal cells. **(I-K)** Double immunofluorescence staining reveals the co-expression of SOX2 and Ki67 in basal cells. **(L)** Quantification of SOX2:Ki67 double positive cells as a proportion of either the SOX2+ or Ki67+ populations in human PCP. Scale bar is 200μm, except in magnified inserts where it is 100μm.

Supplementary Table 1

Genotypes obtained from *Hesx1*$^{Cre/+}$ *x Kras*$^{G12D/+}$ and *Hesx1*$^{Cre/+}$ *x Braf*$^{V600E/+}$ intercrosses

	Genotypes (% Expected)[a]									
	Hesx1$^{Cre/+}$ *Kras*$^{G12D/+}$ (25%)	*Hesx1*$^{Cre/+}$ *Kras*$^{+/+}$ (25%)	*Hesx1*$^{+/+}$ *Kras*$^{G12D/+}$ (25%)	*Hesx1*$^{+/+}$ *Kras*$^{+/+}$ (25%)		*Hesx1*$^{Cre/+}$ *Braf*$^{V600E/+}$ (25%)	*Hesx1*$^{Cre/+}$ *Braf*$^{+/+}$ (25%)	*Hesx1*$^{+/+}$ *Braf*$^{V600E/+}$ (25%)	*Hesx1*$^{+/+}$ *Braf*$^{+/+}$ (25%)	
Stage					Total					Total
10.5 dpc	8	7	8	10	33	6	5	5	8	24
12.5 dpc	10	5	8	3	26	12	10	3	4	29
14.5 dpc	9	5	7	11	32	10	7	8	6	31
18.5 dpc	7	9	3	7	26	10	9	6	7	32
Embryos[†] (% Observed)	34 (29%)	26 (22%)	26 (22%)	31 (26%)	117	38 (33%)	31 (27%)	22 (19%)	25 (21%)	116
Pups[‡] (% Observed)	0 (0%)	10 (36%)	15 (53%)	3 (11%)	28	0 (0%)	7 (32%)	10 (45%)	5 (23%)	22

[a]Derived from expected Mendelian ratios

[†]Chi-square test showed no signifiant deviation from the expected Mendelian ratio in both *Hesx1*$^{Cre/+}$ *x Kras*$^{G12D/+}$ (p=0.6598) and *Hesx1*$^{Cre/+}$ *x Braf*$^{V600E/+}$ (p=0.1596).

[‡]Chi-square test showed a statistically significant deviation from the expected 25% ratio in both *Hesx1*$^{Cre/+}$ *x Kras*$^{G12D/+}$ (p=0.0033) and *Hesx1*$^{Cre/+}$ *x Braf*$^{V600E/+}$ (p=0.0219).

Supplementary Table 2

Digital PCR showing BRAF V600E mutations in human PCP samples

Case No	Diagnosis	[DNA] (Copies/ µL)	BRAF V600E Digital PCR		
			Mean mutant copies/µL	Mean wild-type copies/ µL	Mean % mutant
87	PCP	2087	252.5	655	27.60%
91	PCP	6653	1262.5	3302.5	27.70%
96	PCP	360	36	240	13.00%
97	PCP	262	11.8	72.5	14.20%
101	PCP	1978	122.5	395	23.60%

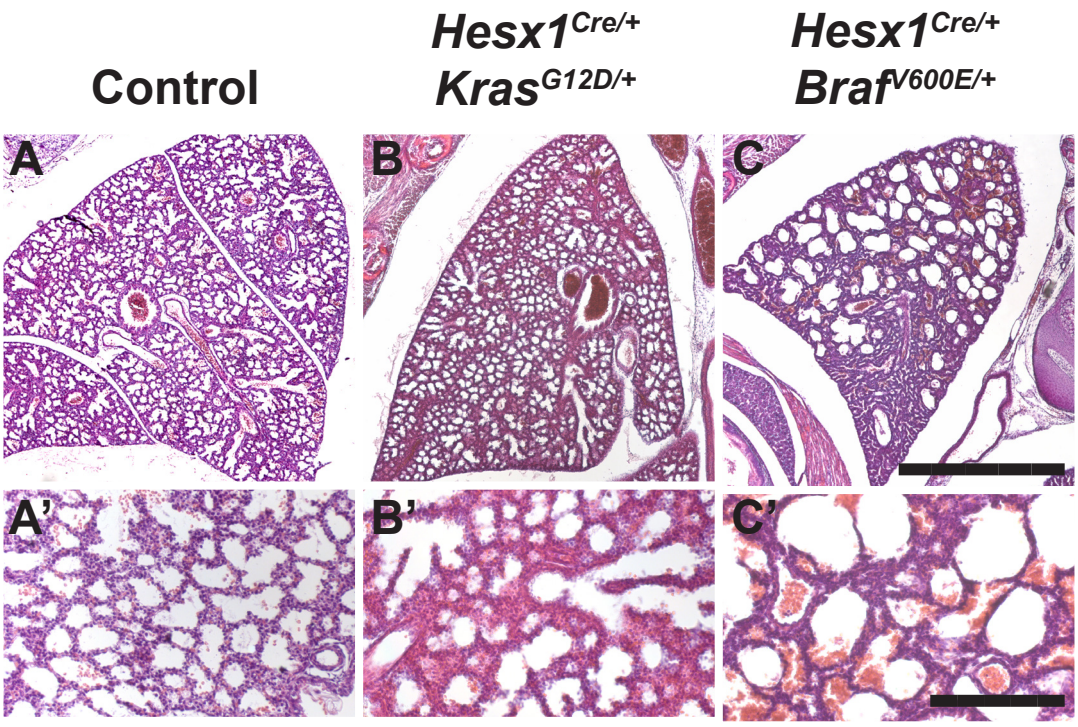

Fig. S1 Abnormal morphogenesis of the lungs in *Hesx1*$^{Cre/+}$;*Braf*$^{V600E/+}$ and *Hesx1*$^{Cre/+}$;*Kras*$^{G12D/+}$ mutants. (A-C) Haematoxylin and eosin staining of lung tissue at 18.5 dpc in *Hesx1*$^{Cre/+}$;*Braf*$^{V600E/+}$, *Hesx1*$^{Cre/+}$;*Kras*$^{G12D/+}$ and control embryos showing expansion of airway structures, which are especially evident in *Hesx1*$^{Cre/+}$;*Braf*$^{V600E/+}$ mutants. Scale bar is 200μm (A'-C') Inserts show higher magnification of terminal airways and alveoli. Scale bar is 100μm.

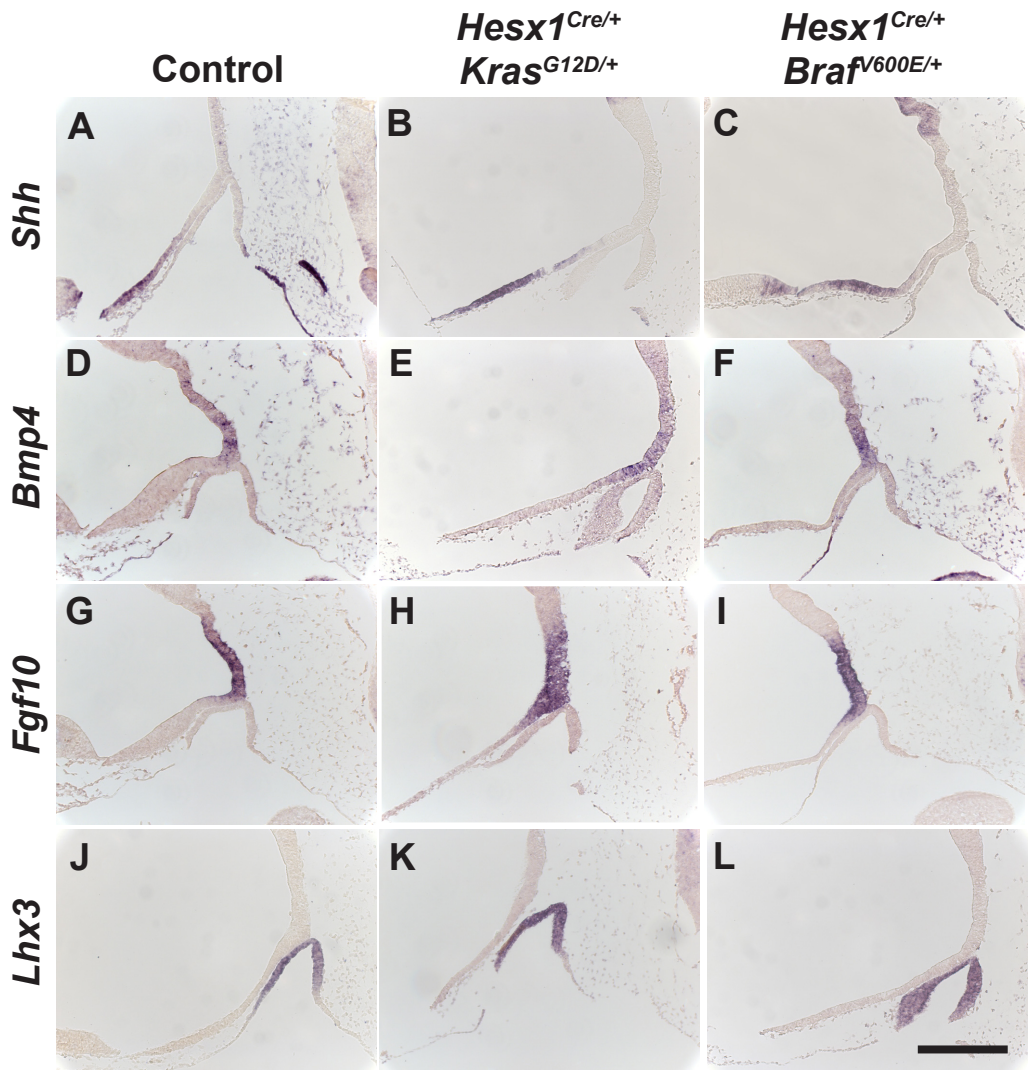

Fig. S2. Normal Rathke's pounch specification in *Hesx1*$^{Cre/+}$;*Braf*$^{V600E/+}$ and *Hesx1*$^{Cre/+}$;*Kras*$^{G12D/+}$ mutants. *In situ* hybridisation on sagittal histological sections of 10.5 dpc embryos; probes and genotypes are indicated. Note the comparable expression of *Shh*, *Fgf10* and *Bmp4* in the prospective hypothalamus and *Lhx3* in Rathke's pouch, between mutant and control embryos. Scale bar is 200µm.

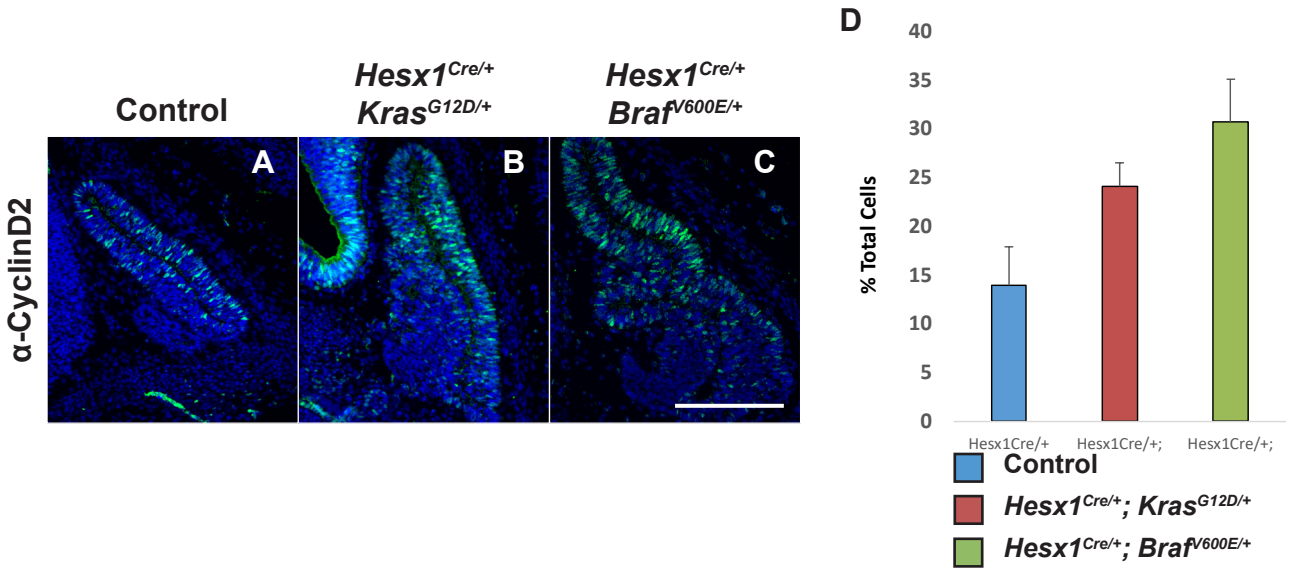

Fig. S3. Increased cyclin D2 expression in *Hesx1*$^{Cre/+}$;*Braf*$^{V600E/+}$ and *Hesx1*$^{Cre/+}$;*Kras*$^{G12D/+}$ mutants. (A) immunostaining on sagittal histological sections revealing the elevated expression of cyclin D2 in the periluminal epithelium of Rathke's pouch in the mutants relative to the control embryo. **(B)** Quantification of cyclin D2+ve cells as a proportion of the total DAPI+ve nuclei of the perilumal epithelium showing a higher proportion of expressing cells in the mutant embryos relative to the controls. Scale bar is 200μm.

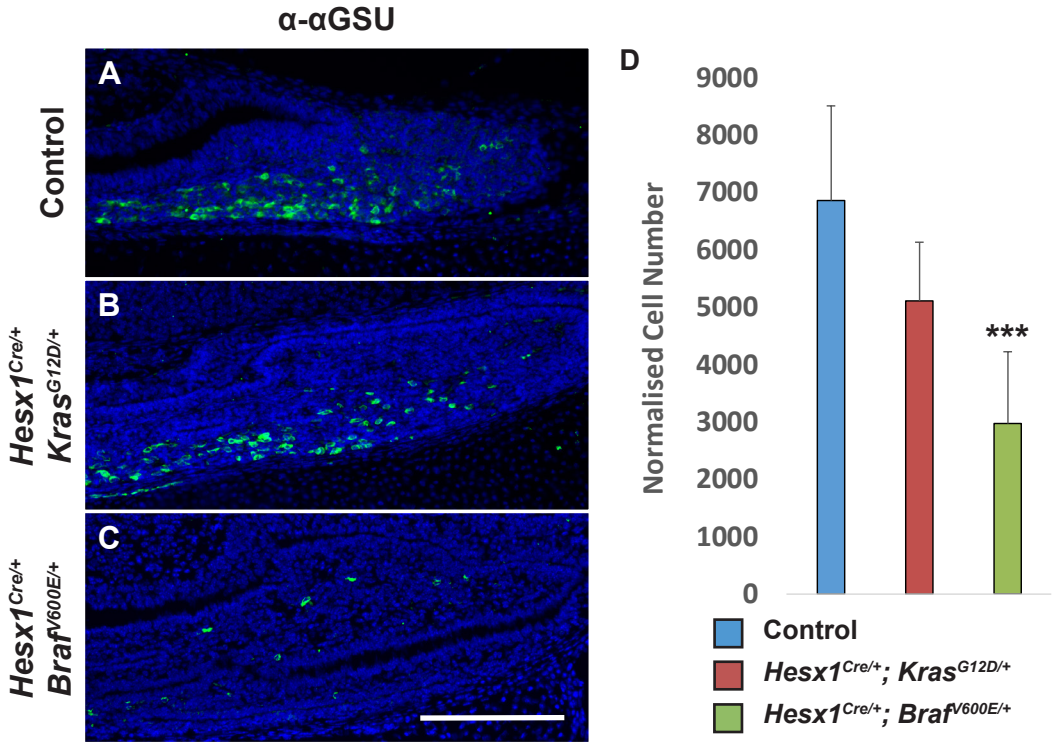

Fig. S4. Reduced αGSU expression in *Hesx1*$^{Cre/+}$;*Braf*$^{V600E/+}$ and *Hesx1*$^{Cre/+}$;*Kras*$^{G12D/+}$ mutants. (A) Immunostaining on transverse histological sections revealing the expression of αGSU in mutants and a control embryo. **(B)** Quantitative analysis of αGSU+ve cells in mutant and control pituitaries revealing a reduction in total numbers of αGSU+ve cells, which reaches statistical significance for the *Braf*-deficient mutant. Scale bar is 200μm.

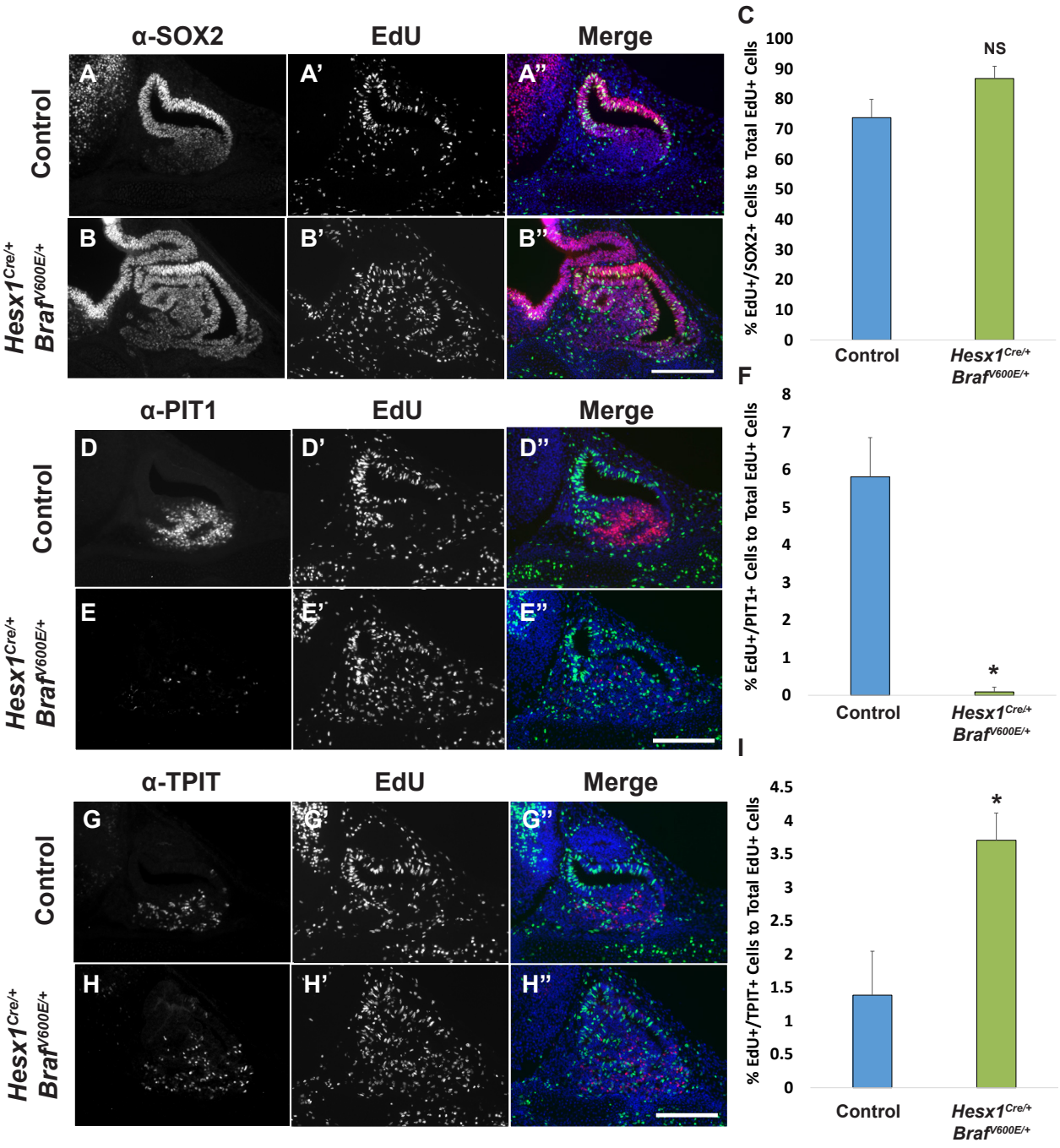

Fig. S5. Proliferation of TPIT+ and PIT1+ progenitor populations are affected in *Hesx1*$^{Cre/+}$*;Braf*$^{V600E/+}$ mutant pituitaries at 14.5 dpc. EdU was administered once to pregnant females at 14.5 dpc and embryos were analysed 2 hours later. (**A-C**) Most of the labels cells are SOX2-positive with a trend towards increased numbers in the mutant pituitaries relative to controls (controls 74%, mutants 87%; p=0.1599). **(D-I)** In the control pituitaries, 6% of the EDU+ cells expressed PIT1 and 1.4% TPIT, whilst in the mutant developing glands, only 0.1% of the EDU+ cells express PIT1 and 3.7% TPIT. Both, the increase in TPIT and decrease in PIT1 progenitor proliferation are statistically significant (p=0.0246, PIT1 and p=0.0490, TPIT). Scale bar is 200μm.

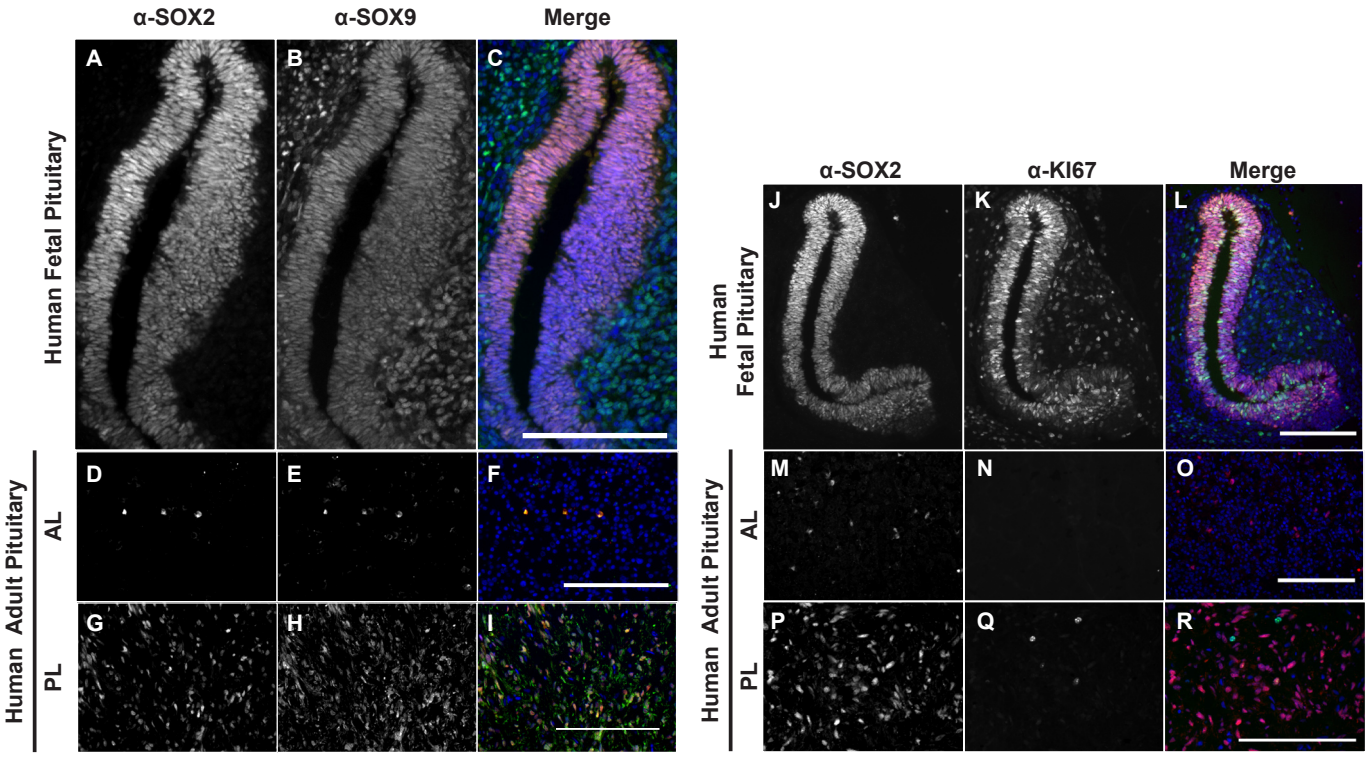

Fig. S6. Expression of SOX2, SOX9 and Ki67 in human fetal and adult pituitaries. Immunostaining on histological sections of human pituitaries, stages and markers are indicated. **(A-I)** At embryonic stage CS20 (A-C), SOX2 and SOX9 are co-expressed in the vast majority of the embryonic progenitors of the developing Rathke's pouch. In contrast, expression of SOX2 and SOX9 is not observed in the adult anterior pituitary (D-F), but there are expressing cells in the posterior pituitary (G-I). **(J-R)** At embryonic stage CS20 (**J-L**), double immunostaining reveals the co-expression of SOX2 and the cycling marker Ki67 in the periluminal progenitors of Rathke's pouch. However, in the adult pituitary, Ki67+ve cells are rare and do not co-localise with SOX2+ve cells in the anterior (**M-O**) or posterior (**P-R**) pituitary, where they are more abundant (**P**). Scale bar is 200µm.